2016

Dynamic Characterization of Naturally Fractured Reservoirs with Fractal Geometry: Methodology of Analysis

Vargas, Lauro

UNIVERSITY OF CALGARY

Dynamic Characterization of Naturally Fractured Reservoirs with Fractal Geometry: Methodology of Analysis

by

Lauro Jesus Vargas Munoz

A THESIS

SUBMITTED TO THE FACULTY OF GRADUATE STUDIES

IN PARTIAL FULFILMENT OF THE REQUIREMENTS FOR THE

DEGREE OF MASTER OF SCIENCE

GRADUATE PROGRAM IN CHEMICAL AND PETROLEUM ENGINEERING

CALGARY, ALBERTA

JULY, 2016

Abstract

Naturally Fractured Reservoirs (NFR) contain over 60% of hydrocarbon reserves in the world. Most NFR have heterogeneities occurring in a wide range of spatial scales. Generally, NFR are modeled using Euclidean geometry with homogeneous fracture systems that work well for some specific cases. However, the presence of fractures at different scales, the non-uniform distribution of fractures, and the connectivity of the fracture network are important factors of uncertainty in reservoir models. Fractal geometry is one of the best ways to take into account heterogeneities present in a porous medium at different scales, their non-uniform distribution in space, and the connectivity of the fracture network.

This thesis puts forward a methodology to identify, validate and define the fractal parameters from NFR. It considers reservoir engineering and geologic information to gain a comprehensive understanding of this type of reservoirs. This methodology was applied to two field cases from the southwest of Mexico.

Acknowledgements

I would like to take this opportunity to express my gratitude and respect to my supervisor Dr. Zhangxing (John) Chen for providing me the opportunity to study at the University of Calgary and for his support in my research.

I am also grateful to my co-supervisor Dr. Rodolfo Gabriel Camacho Velazquez for his help and time during the development of my research; without his helpful discussions and great suggestions, I could not have finished my research on time.

Special thanks go to Bruno Lopez Jimenez and Jaime Piedrahita Rodriguez, for their time, guidance and technical support with respect to different aspects of this thesis.

Financial support provided by Petroleos Mexicanos (PEMEX E&P), Consejo Nacional de Ciencia y Tecnologia (CONACyT), NSERC/AIEES/Foundation CMG IRC in Reservoir Simulation, AITF (iCORE) Chair, and the Department of Chemical & Petroleum Engineering at the Schulich School of Engineering are greatly appreciated.

Finally, I would like to acknowledge my undergraduate studies at Escuela Superior de Ingenieria y Arquitectura, Campus Ticoman at Instituto Politecnico Nacional (IPN), where I learned the basis of petroleum engineering.

Dedication

A las personas que amo:

Mi esposa Carmen y a mi hijo Lauro E.

Mi mamá Hilda

Mi tía Gloria

Kunta y Kizzy

Y al niño que alguna vez fui y que me enseño que los sueños son alcanzables…

Table of Contents

List of Tables

List of Figures and Illustrations

List of Symbols, Abbreviations and Nomenclature

Symbol	*Definition*
A	*Area, ft^2. L^2*
B	*Intercept*
B	*FVF (RB/STB) (res m^3 / stock-tank m^3)*
C	*compressibility, psi $^{-1}$*
C_{ft}	*Total fracture compressibility, psi $^{-1}$*
C_{mt}	*Matrix compressibility, psi $^{-1}$*
dp/dl	*potential gradient in the flow direction*
D	*Euclidean dimension*
d_{mf}	*Fractal dimension*
fBm	*fractional Brownian motion*
fGn	*fractional Gaussian noise*
H	*Hurst exponent*
Hm	*Matrix thickness, ft*
k	*Permeability L^2*
kf	*Fracture permeability, md, L^2*
Kw	*Permeability for fractal reservoirs, md*
K_2	*Fracture permeability, md, L^2*
L	*distance, ft,L*
m_b	*Porosity exponent of the matrix*
m_s	*Mean*
NFR	*Naturally fractured reservoir*
NpD	*Dimensionless Cummulative production*
OOIP $_c$	*Original oil in place , composite system*
OOIP $_f$	*Original oil in place , fracture system*
OOIP $_m$	*Original oil in place , matrix system*
p	*Pressure, psi, m/Lt^2*
p_{c1hr}	*Pressure at 1 hour on last straight line , psi, m/Lt^2*

p_i	*Initial pressure, psi, m/Lt^2*
p_{f1hr}	*Pressure at 1 hour on last straight line , psi, m/Lt^2*
p_{wf}	*Flowing wellbore pressure, psi, m/Lt^2*
pwD	*Dimensionless wellbore pressure*
Pws	*Wellbore pressure at shut- in , psi, m/Lt^2*
Q	*flow rate, STB/D, L^3/t*
qwD	*Dimensionless rate production*
r_w	*Wellbore radius, ft*
Rt	*Total resistivity (ohm–m)*
Rw	*Water resistivity (ohm–m)*
R/S	*Rescaled range analysis*
S	*Skin factor*
S_f	*Fracture storage (ft/psi)*
S_m	*Matrix storage (ft/psi)*
So	*Oil saturation, fraction*
Sw	*Water saturation, fraction*
Sof	*Fracture oil saturation, fraction*
S_{om}	*Matrix oil saturation, fraction*
S_{wf}	*Fracture water saturation, fraction*
S_{wm}	*Matrix water saturation, fraction*
T	*Time, hours*
Tc	*Time to the initial pressure, hours*
t_D	*Dimensionless time*
T_f	*Fracture transmissivity (md/ft)*
V	*Apparent flow velocity, (cm/sec).*
Δp	*pressure differential, psi*
Δt	*Delta time , hours*
Θ	*Connectivity index*
Δ	*Spectral dimension*
Γ	*Gamma function*

ϕ	*Total porosity, fraction*
ϕ_b	*Matrix porosity, fraction*
Φ_2	*Fracture porosity, fraction*
Σ	*Standard deviation*
η_c	*Composite hydraulic diffusivity for strata*
η_g	*time –dependent hydraulic diffusivity*
μ	*viscosity of the fluid, cp, m/Lt*^{2}
Ω	*Storage capacity coefficient*

Chapter One: **INTRODUCTION**

Reservoir engineers analyzed NFR by considering that all of them have Euclidean geometry (a term used to define the conventional geometry). In reality their nature is very complex; for instance a fracture network in an oil reservoir may have many patterns of irregular nature with a non-uniform distribution. For these reasons, its geometry is not Euclidean.

Objects with a non-Euclidean geometry are presented in many science fields and petroleum engineering is not an exception. A fractal dimension plays a central role in this research. A fractal dimension is a concept that was introduced in 1918 by Felix Hausdorff [32], and Benoit B. Mandelbrot invented the term "fractal" in 1975, which is derived from the Latin word "fractus". The corresponding Latin verb frangere means "to Break" to create irregular fragments [32].

A great revolution of ideas separates the classical mathematics of the 19th century from the modern mathematics of the 20th. Classical mathematics had its roots in the regular geometric structures of Euclid and the continuously involving dynamics of Newton. Historically the revolution was forced by the discovery of mathematical structures that did not fit Euclidean patterns and the dynamics of Newton. These new structures were regarded as pathological, as a "gallery of monsters", or a kind of cubist painting and atonal music that were upsetting established standards of taste in the arts at about the same time.

As Mandelbrot indicated, Nature has played a joke on mathematicians. The 19th-century mathematicians may have been lacking in imagination, but Nature was not.[32]

The basics of fractals are dimensionally discordant and can serve to transform the concept of fractals from an intuitive to a mathematical one. Mandelbrot stated that the more intuitive of the two is the topological dimension according to Brower, Lebesgue, Menger and Urysohn.[32] The first one is denoted by DT (Topological Dimension) and the second one is denoted by D (Fractal Dimension). The dimension DT is always an integer, but D does not need to be an integer and the two dimensions do not need to coincide.

"A fractal is by definition a set for which the Hausdorff Besicovith dimension strictly exceeds the topological dimension, every set with a noninteger D is a fractal.[32]"

The topology, which used to be called geometry of situation or analysis in situ, refers to Euclidean geometry. Two objects are equivalent if they transform into each other through rotations, translations, and reflections. Thus, the angle, area, length and, volume measurements and others remain the same, without breaking or separating what was united, or paste what was separated. They must have the same number of pieces, holes, and intersections. Most fractals are invariant under certain transformation of scale. They are called scaled. A fractal invariant under ordinary geometric similarity is called self-similarity. Figure 1-1

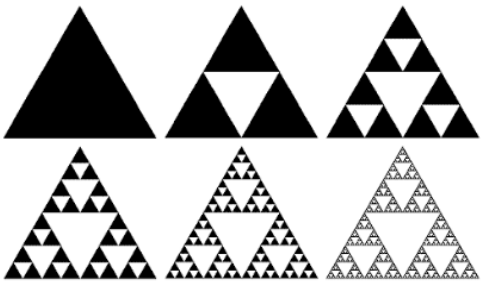

Figure 1-1: Sierpinski triangle, self-similarity example.

Figure 1-2: Shows some examples of fractal geometry taking examples from different sciences where the fractal geometry is analyzed.

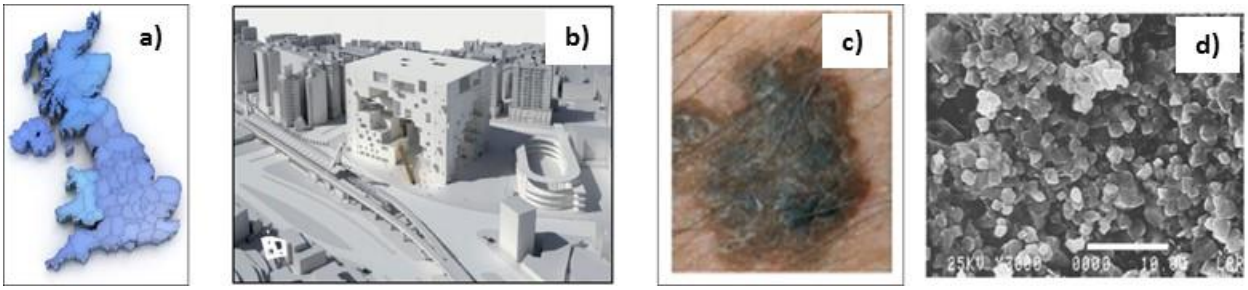

Figure 1-2: The Coast of Britain. (b) Taipei Performing Arts Center Building. (c) Skin Cancer Sample. (d) SEM Image Smackover limestone.

Nowadays, there is not a methodology to develop an initial dynamic characterization and compute fractal parameters from NFR with fractal geometry; resulting in impossibility to establish the best strategy for the field development. This consequence is reflected in unproductive wells, very optimistic production forecasts and inefficient primary, secondary and enhanced oil recovery methods. The intention of this research was focused in establishing such a methodology. First, the fractal parameters (fractal dimension and connectivity index) can be computed. Second, two equations were proposed to compute a

skin factor and permeability. Finally, the influence of fractal parameters on production performance was evaluated. Based on this methodology an initial dynamic characterization can be developed in order to define the best strategy for the field development.

Chapter Two: **BACKGROUND ON NATURALLY FRACTURED RESERVOIRS**

2.1 Introduction

In order to understand the dynamic behavior of NFR, it is important to know their geologic aspects and to consider all the direct and indirect information available for the field being studied. Many reservoir engineers, including myself, argue that there is a mistake in the way that a characterization of a NFR is developed, because each specialist (geologist, geophysicist or petrophysicist) gives their own conclusion and sometimes that conclusion does not agree with other information from the field such as wireline logs, bottom hole pressure behavior, production history, and cores. This situation has caused incorrect decisions when a development strategy for the field is proposed, resulting in unproductive and low productivity wells and unsuccessful process of additional recovery because the information of a reservoir simulation model yields unreal forecast.

As a reservoir engineer, it is necessary to consider all the information available. We have the commitment to ask each specialist about their results and how their conclusion can be supported by each other's knowledge because at the end of the day, the goal for all of us is the same: to increase the oil and gas recovery factors of the field. After this personal comment, we start with the main geologic aspects of NFR taking as a reference the notes from the class of Professor Roberto Aguilera (Naturally Fractured Reservoir the University of Calgary).

2.2 Geology

Development of a reservoir description is based on "Rock Studies", which are important in order to find a relationship between rock properties, such as porosity, horizontal and

vertical permeability, water saturation and capillary pressure, and rock types. These are linked with lithology, facies, and geological depositional environment. Rock properties are not the results from random geological events, but rather a reflection of the combination of different lithologies and depositional environments. Thus, the first step to develop a reservoir description is focused on correlating rock properties and rock types given by a combination of depositional environment, lithologies and facies.

First, information from reservoir rocks must be gathered and analyzed. Rock properties come from different information sources such as cores (small samples and full diameter lab tests), cuttings, and well log analysis, which can be the most important. Secondly, the lab tests are run following standard guides, e.g., RCA – routine core analysis and SCAL – special core analysis. Lithology, facies and geological depositional environment, are conducted by using core descriptions and core analysis, such as thin sections, X diffraction ray (XDR) and SEM (scanning electron microscopy), master logs (cutting geological description while drilling operations), and drilling events (e.g., a mud loss can be a clue of natural fractures).Finally, this information is put together in order to obtain a correlation between rock properties and lithology, facies and depositional environment, for instance, a grain size, sorting, cross-bedding, natural fractures, vuggy and fining-up or coursing up sequence [3].

2.3 Genesis of a NFR

According to Stearns (1990), a natural fracture is a discontinuity that results from stress that exceeds the rupture strength of rock, and Nelson (1985) defined it as a naturally occurring macroscopic planar discontinuity in rock due to deformation or physical

diagenesis[3].Landes and Nelson (1985) listed several causes for the generation of a natural fracture:

- Structural deformation associated with folding and faulting tend to generate cracks along fault line which produces a zone of dilatancy. This one is probably responsible for a large part of the migration and accumulation of petroleum in fractured reservoirs (Mead, 1925; McNaughton, 1953). (Figure 2-1).

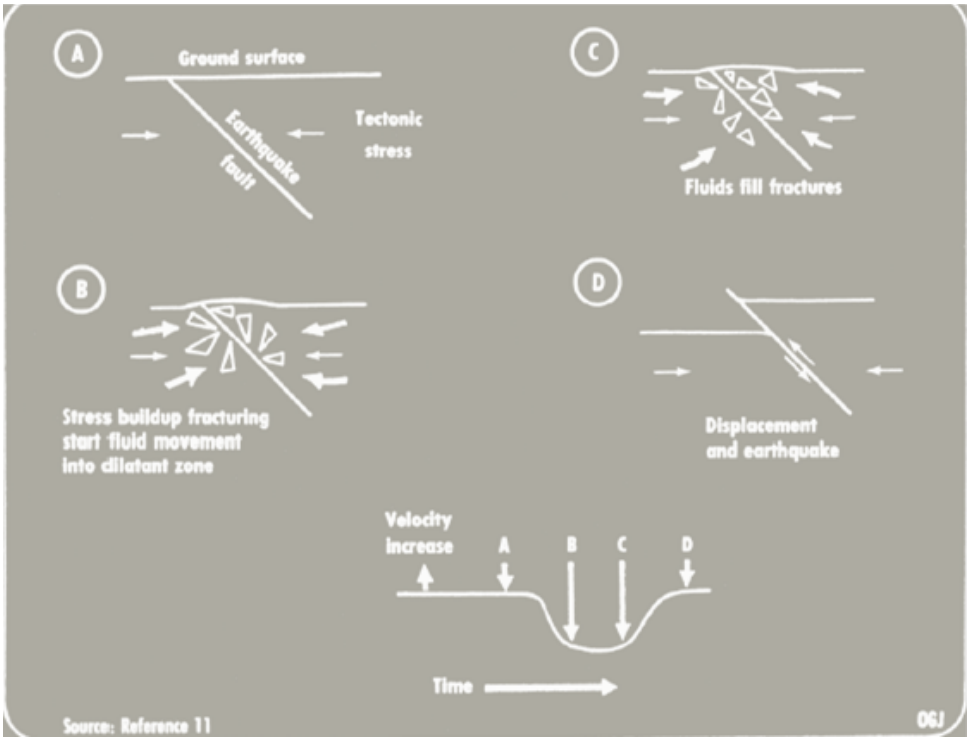

Figure 2-1: Migration and accumulation in natural fractures-Dilatancy fluid model, Servipetrol LTD. Canada (2011).

- Rapid and deep erosion of overburden permits expansion uplift and fracturing along planes of weakness.

- Volume shrinkage due to dewatering in shales, cooling of igneous rocks, or desiccation in sedimentary rocks.
- Paleokarstification and solution collapse as suggested by cores analysis of the Brown zone in the Healdton and Cottonwood Creek fields in Oklahoma (Lynch et al 1990).
- Fracturing through release of high pore –fluid pressure in geopressured sedimentary strata (Hubbert and Willis, 1957; Capuano, 1993).
- A rare meteorite impact causes complex, extensively brecciated, and fractured reservoirs (Kuykendall et al, 1994).

2.4 Classification

From the classification of a NFR from a ***geologic point of view*** according to D.Stearns, M. Friedman and R.Nelson (1985), the hydrocarbon production is obtained from tectonic fractures followed by regional fractures. For contractional fractures, the surface related fractures are not important for hydrocarbon production. These types of fractures are described as follows:

- Tectonic fractures (fold and fault related) - Tectonic fractures are those whose origin can be attributed to or associated with a local tectonic event on the basis of orientation, distribution and morphology. As such, they are developed by the application of surface or external forces (Nelson, 1985).
- Regional fractures- They are developed over large areas of the earth crust with relatively little change in orientation , show no evidence of offset across a fracture plane, and are always perpendicular to major bedding surfaces (Stearns, 1972, Nelson, 1975).

- Contractional (diagenetic) fractures- This group is a collection of fractures of varying origins. Each is an extension fracture associated with either a general bulk volume reduction throughout the rock due to desiccation or a thermal gradient.
- Surface related fractures.

Fractures can have a positive or negative influence on the fluid flow. For this reason, it is important to consider the magnitude and direction of in situ stresses, strike, dip and spacing of the fractures, matrix and fracture porosity, matrix and fracture permeability, and matrix and fracture water saturation. This information is going to help to define how the in-place hydrocarbons are distributed between matrix and fractures, and the flow capacity of wells. It is important to consider the rock morphology (the face of cores) and identify the effect of the fracture intensity or fracture spacing, petrology (composition, a grain size, matrix porosity and permeability), and geometry (bed thickness-net pay and structural position).

The classification of a NFR from a *storage point of view* is regarded to the matrix and the characterization of natural fractures as types A, B and C. This classification was published originally by McNaughton (1975). The presence of fractures is important to obtain wells with commercial success. Figure 2-2.

- ***Type A:*** The bulk of the hydrocarbon storage is in the matrix and a small amount of storage in fractures. The matrix typically has a very low permeability while the natural fractures tend to have a much larger permeability. In this case, the fractures may have a negative effect in a reservoir because they facilitate unwanted water channelling.

- ***Type B:*** Approximately half of the hydrocarbon storage is in the matrix, and half is in the fractures. The matrix is tight and the fractures are much more permeable than the matrix.
- ***Type C***: All the hydrocarbon storage is in the fractures with no contribution from the matrix. In this case, the fractures provide storage and permeability to generate hydrocarbon production.

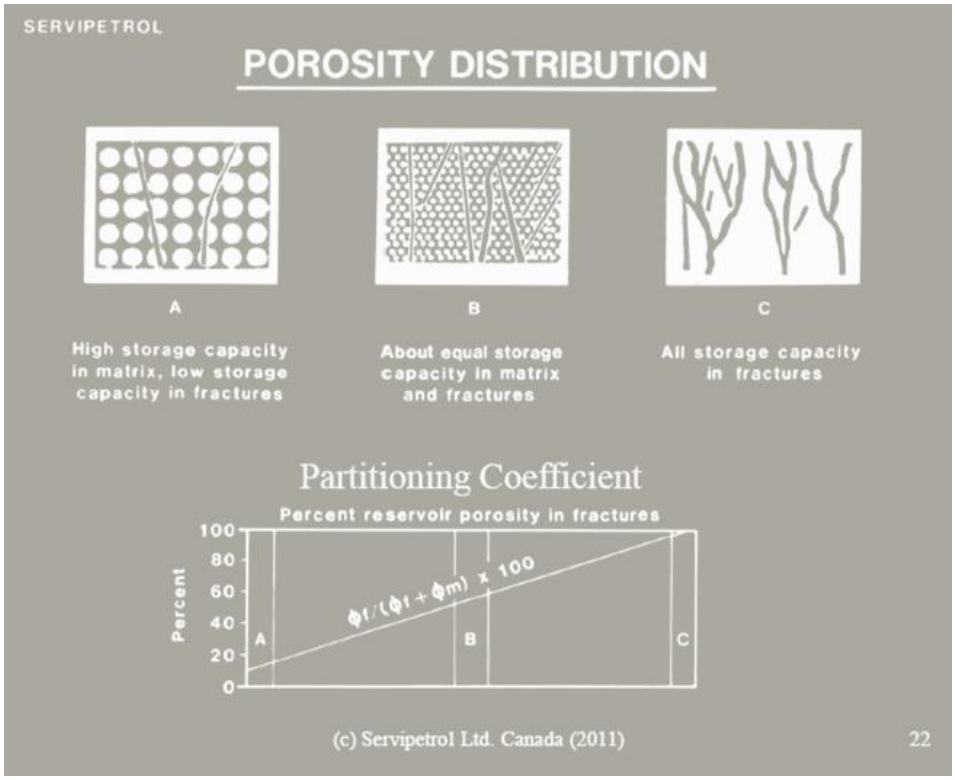

Figure 2-2: Storage Classification for NFR, Servipetrol LTD. Canada (2011).

The relative permeabilities in NFR have a different behavior than those in the conventional ones. For the reservoir type B, where the ideal combination exists in porosity and permeability, the relative permeability curves for the fractures present straight lines with a

45° angle. It means that the fracture system is like tubes, where the irreducible water and residual oil saturations are equal to zero. This must be taken into account when a reservoir simulation model is developed in order to generate reliable forecasts Figure 2-3.

In the case of the reservoir type C, where the matrix system is not a good reservoir rock and even if there is some matrix porosity, the fractures have only a fraction of the total porosity, but they will have 100 % of the hydrocarbon storage capacity Figure 2-3.

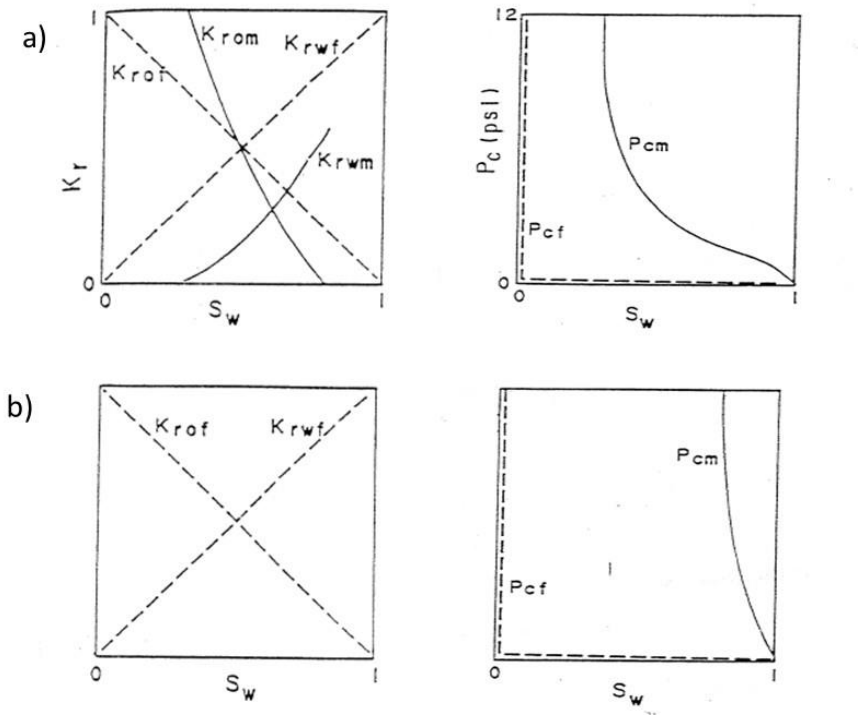

Figure 2-3: (a) Type B reservoir; Relative permeability (Kr) and capillary Pressure (Pc) curves. (b) Type C reservoir; Relative permeability curves, subscripts o, w, m and f stand for oil, water, matrix and fractures (after Aguilera, 1983).

The classification of a NFR from a ***pore classification point of view*** is based in the definition of the geometry of pores and a pore size. With this information, it is possible to estimate the productive characteristics of the reservoir. This classification was proposed by Coalson et al. (1985).

The pore size can be recognized by applying different techniques, for example, by Winland r_{45} and Aguilera rp_{35} (pore throat aperture at 35 % Hg saturation during a capillary pressure injection test) Figure 2-4.

$$rp_{35} = 2.665((k|100 * \phi))^{0.45} \quad 2\text{-}1$$

where: k (md), ϕ (fraction)

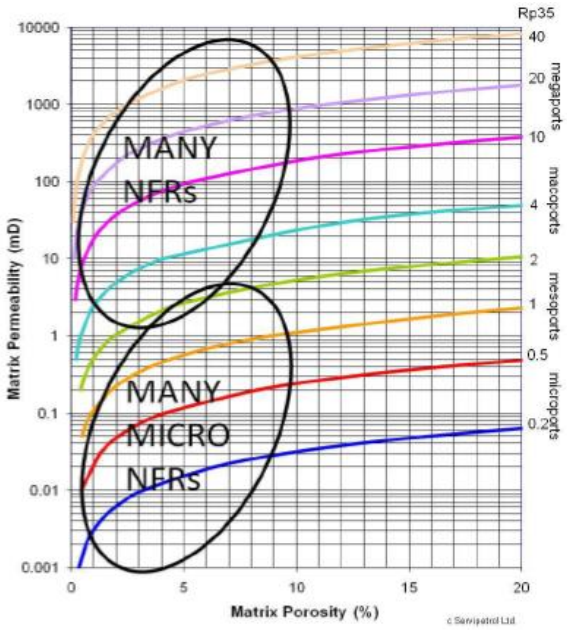

Figure 2-4: Aguilera rp35 (microns), Servipetrol Ltd. Canada (2014)

Table 2-1shows that according to the value of calculated rp_{35} it is possible to estimate the port size and the barrels expected per day, dependent on the formation thickness.

Table 2-1: Possible oil rates by port size, (Martin, Solomon and Hartmann, 1997), Servipetrol Ltd. Canada (2014)

Port size	rp_{35} (μm)	Oil rate (barrels per day)
Megaports	>10	10,000
Macroports	2 to 10	1,000
Mesoports	0.5 to 2	100
Microports	0.2 to 0.5	10
Nanoports	< 0.2	Mostly seal

2.5 Basic definitions

Fracture morphology is focused on the form of natural fractures, which means that they are open, deformed, mineral filled and vuggy fractures (Nelson, 1985). Cores can give us an idea of the type of a matrix and fracture interaction. This is very important if we are considering oil recovery factors [3].

When fractures are open and the secondary mineralization is not considerable, the hydrocarbon flow from the matrix to the fractures in an *unrestricted manner*. This is called *no secondary mineralization.* The reservoirs with these characteristics have wells with high initial oil rates. These fractures tend to close when a reservoir is depleting due to the in situ stress and initial reservoir pressure. For this reason, it is important to consider the

compressibility of fractures when an oil – gas forecast is proposed in order to obtain realistic production predictions.

For fractures that have some *secondary mineralization* the interaction of the matrix and– fractures is in a *restricted manner*. In this case, the fracture closure is reduced by the presence of the mineralization. A skin related to this is identified in a well pressure transient test, and is considered natural, not a mechanical skin. In the case of fractures with a *complete secondary mineralization*, the oil – gas recovery factor will be decreased. This condition is not desirable when a reservoir is under development because it affects the economics of the project.

The vuggy fractures increase permeability, and, therefore, the production expected from this type of fractures is high. In the case of connected vugs, primary flow can exist through both fracture and vug networks.[4] It is important to define the secondary porosity and secondary permeability, because both play an important role when we are considering NFR.

Let us start with the basic definition of *permeability*, which is a property of a porous medium and is a measure of the capacity of the medium to transmit fluids.

A NFR is focused on primary permeability which is related to the matrix and secondary permeability related to fractures and/or vugs.

The *matrix permeability* is obtained by the Darcy law:

$$v = -\frac{k}{\mu} \times \frac{dp}{dl} \qquad 2\text{-}2$$

where:

v=apparent flow velocity, (cm/sec).

μ=viscosity of the fluid, cp.

dp / dl= potential gradient in the flow direction, atm/cm.

k=permeability of the rock, Darcys.

It is important to present the assumptions for the applicability of the Darcy law:

- Laminar flow
- Pore space saturated 100% with a flowing fluid

The Darcy law in petroleum field units:

$$q = \frac{0.001127kA\Delta p}{\mu L} \qquad 2\text{-}3$$

where:

q=flow rate, b/d

k=permeability, md

A=area, sq ft

Δp=pressure differential, psi

μ=viscosity, cp

L=distance, ft

The fracture permeability is a scale dependent property. When considering the fracture width (*Wo*) in inches, the intrinsic permeability of fractures in Darcy is given by the following equation:

$$k_f = 54 \times 10^6 \ Wo^2 \ [Darcy] \qquad 2\text{-}4$$

The fracture permeability from Equation 2-4 is associated to single point properties, and the following equation can be applied to the bulk properties of the reservoir.

$$k_2 = \frac{k_f W_o}{D} \qquad 2\text{-}5$$

where:

D= distance between fractures

Secondary porosity. It is an induced porosity, and is the product of a geologic process occurring after deposition. This has no direct relation to the form of sedimentary particles. It occurs due to solution, recrystallization, and dolomitization of fractures and vugs. The fracture porosity reported in the literature is in the range of 1 and 10%. The vug porosity can be much higher than the fracture porosity.[4]

2.6 Pickett plot applications

The OOIP (original oil in place) is the most important calculation to start a development strategy of any reservoir. For this, the Pickett plot analysis is very useful to define the type of NFR, the fracture porosity, the partitioning coefficient *(v)* and then define the OOIP in fractures and the matrix. This methodology, explained by Dr. Aguilera, is important when an initial characterization is developed for these types of reservoirs. In our experience,

when an OOIP is calculated, a partitioning coefficient is not part of the analysis and even the porosity exponent is not analyzed in order to determine the type of NFR.

The input data for this analysis is the porosity exponent of the matrix *(mb)*, the value of the constant *(a)*, the oil volume factor, the water oil ratio value, the values of each zone of the true resistivity, total porosity and the thickness of each region.

The first step is to build a Pickett plot following the next steps Figure 2-5:

- Create a log log plot, using the total porosity and the total resistivity.
- Identify the points with a tendency of a straight line, which corresponds to 100% of water.
- Identify the points which do not have a tendency, these points correspond to the oil zone and Figure 2-5 identifies the water and oil zones.

Water resistivity *(Rw)*: In order to obtain the R_w the straight line is identified, 100% water is followed until the total resistivity axis (Figure 2-5), and then from the following equation: R_w can be calculated.

$$R_t = a\, R_w \qquad 2\text{-}6$$

Composite porosity exponent *(m)*: In the case of the calculation of *m* the data which corresponds to the 100 % water zone identified in the Pickett plot is considered and then the slope of this line is calculated (Figure 2-5). The value of this slope is the porosity exponent. The value of the porosity exponent of a composite system *(m)* and the value of the porosity exponent of the matrix *(mb)*, are compared for this example. The value of *m*

is= 1.59 and the value of mb given is 2 (a value obtained from laboratory tests); this means that m is less than *mb*, which corresponds to a naturally fractured reservoir. For most consolidated rock the value of *m* is greater.

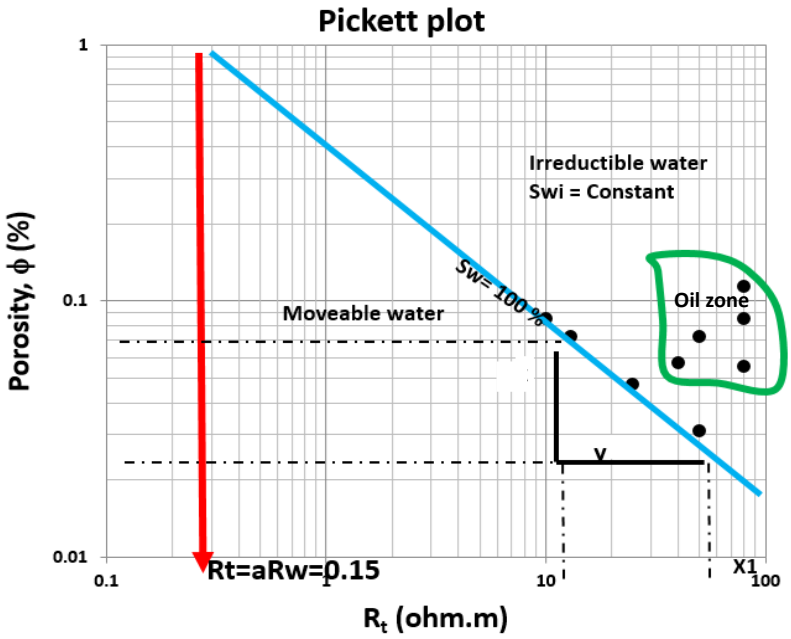

Figure 2-5: Pickett plot after Aguilera, 1990.

The next step is the calculation of the fracture porosity *(ϕ_2)*, matrix porosity *(ϕ_b)* and the partitioning coefficient (v), using the following equations:

$$m=\log (v\phi+ (1-v\phi)\ \phi_b{}^{mb}) / \log \phi \qquad 2\text{-}7$$

$$\phi_2 = v\ \phi \qquad 2\text{-}8$$

$$\phi_b = (\phi- \phi_2) / (1- \phi_2) \qquad 2\text{-}9$$

where:

m= porosity exponent of composite system of matrix and fractures

m_b= porosity exponent of the matrix

ϕ=total porosity, fraction

ϕ_b=matrix porosity of unfractured plug, fraction

ϕ_2=fracture porosity, fraction

v=partitioning coefficient

According to the values of ϕ_b and $\phi_{2\ calculated}$ it is possible to define the type of reservoirs according to their storage point of view.

With this information, the estimation for the original oil in place (OOIP) for the composite matrix and fracture system can be calculated using the following equations:

$OOIP_c$ for composite system

$OOIP_c$= ((7758) (A) (h) (ϕ) (1-Sw)) / (Boi), (barrels) 2-10

$OOIP_f$ for fracture system

$OOIP_f$ =$OOIP_c$ (v), (barrels) 2-11

$OOIP_m$ for matrix system

$OOIP_m$= $OOIP_c$ - $OOIP_f$, (barrels) 2-12

As previously noted, this information and the initial calculations for a NFR must be considered when the fractures are considered.

Chapter Three: **SEMILOG STRAIGHT LINE ANALYSIS FOR NATURALLY FRACTURED RESERVOIRS**

3.1 Introduction

This chapter follows the research published by Dr. Roberto Aguilera, University of Calgary, based on the SPE paper #13663.

Since 1960, the research of naturally fractured reservoirs has considered Euclidean geometry (model made of orthogonal, equally spaced fractures), where the main premise is that the fracture density is uniform, only one scale is present and all the fractures are connected, Figure 3-1. The characteristic pressure transient response of such models in a 2D space is the classical semi logarithmic behavior. In this case, a radial flow is developed, and the following authors focused on the analysis of the pressure transient response in these type of reservoirs: Barenblantt, G.I. and Zheltov, I.P. (1960) assumed pseudo steady - state interporosity flow in a model made of uniformly distributed fractures. Warren, J.E. and Root, P.J. (1963) considered orthogonal, equally spaced fractures and concluded that a conventional semilog plot of pressure vs time should result in two parallel straight lines with a transition period in between. Abraham de Swaan (1976) developed a diffusivity equation and analytic solutions to handle unsteady - state interporosity flow; however, he could not analyze the transition period between the two parallel straight lines. Najurieta, H.L. (1980) developed approximate analytical solutions of Swaan's radial diffusivity equation, which could handle the transition period between, the first and last straight lines. Serra at el (1983); established a stratum model for the cases in which the storativity ratio was smaller than 0.0099.

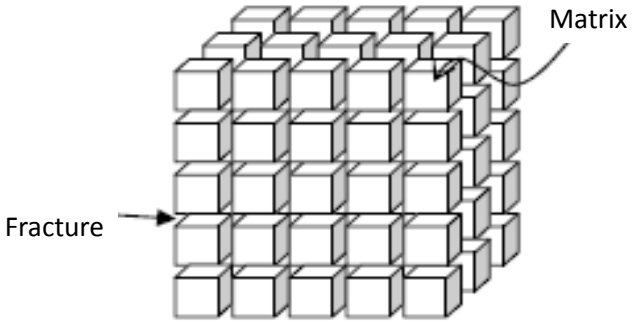

Figure 3-1: NFR model by Warren and Root

3.2 Model consideration

The methodology considers three different shapes of a naturally fractured reservoir: stratum, cubes and matchstick models Figure 3-2.

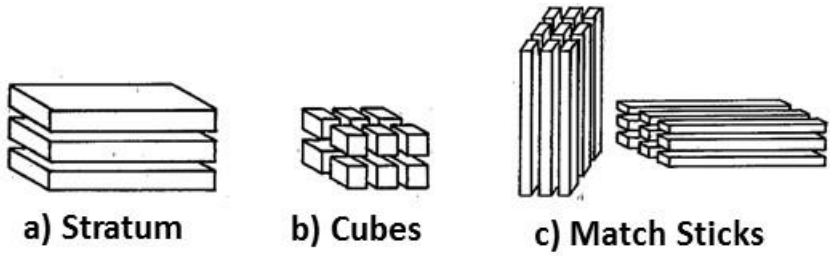

Figure 3-2: a) NFR stratum model, b) NFR cubes model, c) NFR matchstick model.

Stratum model: Represents a uniformly fractured, stratified reservoir with a distance between fractures equal to h_m. From a geological point of view, this model represents shallow reservoirs less than 2500 ft or a deep reservoir dominated by thrust faulting.

Cube model: Represents a uniformly fractured reservoir made of cubes with space in between. The size of each matrix block is h_m and the spaces represent the fractures. From

a geological point of view, this model is an idealization of a reservoir with regional or tectonic shear fractures cut by horizontal fractures.

Matchstick model: Represents a uniformly fractured reservoir made of rectangular parallelepipeds separated by two orthogonal fractured planes. From a geological point of view, this model represents a reservoir with regional or tectonic shear fractures that are not cut by horizontal fractures.

The fluid movement toward a wellbore occurs only in fractures. This assumption can be developed by drawing the matrix blocks from the composite system; the matrix effects on pressure changes in the fractures are taken into account by considering the variable of sources or sinks in the fracture medium. The pressure distribution (Darcy units) in the fractures is given by de Swaan's diffusivity equation, under the conditions of radial, slightly compressible flow plus matrix blocks and outflow injection in the fractures, the pressure equation in the fracture medium is shown in the following equation [16].

$$\frac{\mathrm{k}_f}{\mu}\frac{\delta^2 \Delta p_f}{\delta r^2} = \phi_f\, c\, \frac{\delta \Delta p_f}{\delta t} - q_{ma}\,(\Delta_{pf}, t) \qquad 3\text{-}1$$

where:

The last term is the flow provided by the matrix blocks as the pressure is lowered at their surfaces. The initial and boundary conditions are [16]:

$$\Delta p_f = 0, t = 0$$

$$\frac{\partial \Delta p_f}{\partial r} = \frac{q\mu}{2\pi r_{wh_f k_f}} \quad , \quad r = r_w\,, t \geq 0 \qquad 3\text{-}2$$

and

$$\Delta \mathrm{p_f} = 0, \mathrm{r} \to \infty \qquad 3\text{-}3$$

An approximate solution in field units of Equation 3-1 in the case of an infinite-acting reservoir considering a skin factor is expressed in the following equation:

$$\Delta p = 70.6\frac{qB}{T_f}Ei(-\frac{r^2}{0.00105\eta_g t} + 2s) \quad 3\text{-}4$$

where η_g is the time dependent hydraulic diffusivity given by:

$$\eta_g = \frac{T_f}{S_f + S_m f(t+\tau)} \quad 3\text{-}5$$

The composite hydraulic diffusivity for strata η_c is calculated as a function of the geological characteristics of reservoirs, based on the models mentioned above.

For a stratum model the following equation can be applied:

$$\eta_c = \frac{T_f}{S_f + S_m} \quad 3\text{-}6$$

while for matchsticks it becomes:

$$\eta_c = \frac{2T_f}{2S_f + S_m} \quad 3\text{-}7$$

For cubes it becomes:

$$\eta_c = \frac{3T_f}{3S_f + S_m} \quad 3\text{-}8$$

The equation for matchsticks indicates that there are twice as many fractures per reservoir unit volume than in the stratum case. For a cubic model, the equation indicates that there are three times more fractures than in the stratum model.

The fracture transmissivity T_f is related to the transmissivity of all the fractures intercepting a wellbore, defined by the following equation:

$$T_f = \frac{162.6qB}{m} \quad 3\text{-}9$$

The storage capacity coefficient *(ω)* is the fraction of the total storage within the fractures and can be calculated based on geological characteristics of a reservoir:

For the stratum model:

$$\omega = \frac{S_f}{S_f+S_m} = 10^{-Dp/m} = \frac{t_1}{t_2} = \frac{\eta_c}{\eta_f} = e^{2(s-s_p)} \quad 3\text{-}10$$

For the matchsticks model:

$$\omega = \frac{2S_f}{2S_f+S_m} = 10^{-Dp/m} = \frac{t_1}{t_2} = \frac{\eta_c}{\eta_f} = e^{2(s-s_p)} \quad 3\text{-}11$$

For the cube model:

$$\omega = \frac{3S_f}{3S_f+S_m} = 10^{-\frac{Dp}{m}} = \frac{t_1}{t_2} = \frac{\eta_c}{\eta_f} = e^{2(s-s_p)} \quad 3\text{-}12$$

The variables t_1 and t_2 correspond to the defined times in the first straight line and in the last straight line, respectively, related to the same bottom hole pressure from a semilog plot. The variables η_c and η_f are the hydraulic diffusivities of the composite and fracture systems, respectively. D_p is the vertical separation between the parallel straight lines and S_p is the pseudoskin calculated from the first straight line. Most proven naturally fractured reservoirs tend to have a value of ω=0.0099. If the value of ω is big, then it can be inferred that large production rates can be presented in a reservoir (Figure 3-3).

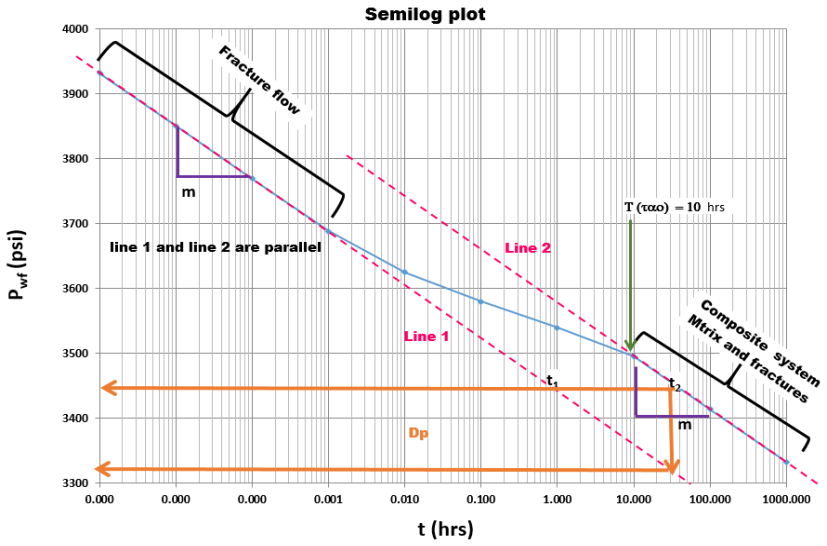

Figure 3-3: Semilog plot (bottom hole pressure vs time) from an assignment NFR class.

The skin effect(s) is calculated from the following equation [4]:

$$s = 1.151\left[\frac{p_i - p_{c1hr}}{m} - \log\left(\frac{\eta_c}{rw^2}\right) + 3.23\right] \qquad 3\text{-}13$$

From the analysis based on the last straight line (composite system), the skin factor can be calculated [4]:

$$s = 1.151\left[\frac{p_i - p_{f1hr}}{m} - \log\left(\frac{\eta_f}{rw^2}\right) + 3.23\right] \qquad 3\text{-}14$$

The size of matrix blocks *(h_m)* The values obtained for h_m from well test analysis should be taken only as orders of magnitude (Equation 3-15); it is important to mention that additional information such as geological models, logs and cores are necessary to better understand this variable.

$$h_m = \left(\frac{\eta_m}{2370}\right)^{1/2} \quad 3\text{-}15$$

where:

$$\eta_m = \frac{k_m}{\phi_m \mu C_{m\tau}} \quad 3\text{-}16$$

τ: time in hours, beginning of the last straight line (Figure 3-3).

Fracture porosity (ϕ_2): This property is attached to bulk properties (Equation 3-17).

Fracture porosity (ϕ_f): This property is attached to a single point property and usually approaches 100%.

$$\phi_2 = \frac{T_f}{\eta_f C_{f\tau} h_m} \quad 3\text{-}17$$

where (C_{ft}) is the total fracture compressibility (Equation 3-18):

$$C_{ft} = S_{of} c_o + S_{wf} c_w + c_f \quad 3\text{-}18$$

The matrix compressibility (C_{mt}), (Equation 3-19) is

$$C_{mt} = S_{om} c_o + S_{wm} c_w + c_{Rock} \quad 3\text{-}19$$

3.3 Straight line analysis

NFR with Euclidean geometry are analyzed based on a semilog plot with two straight lines (composite and fracture systems). In reality, the time duration of buildup and drawdown

tests is short, and only one system can be defined. In this case, the methodology was developed (SPE 13663), and then the storage capacity coefficient *(ω)* and the fracture storage *(S_f)* were calculated.

This analysis was based on a semilog plot (bottom hole pressure vs time); the procedure was as follows, Figure 3-4:

1. Extrapolate the last straight line to the initial bottom hole pressure and read the time t_c

2. Calculate the differential time*(Δt)*; at the initial bottom hole pressure:

$$\Delta_t = \frac{S_m r_w^2 10^{(3.228)}}{T_f} \qquad 3\text{-}20$$

3. Calculate the fracture storage:

$$S_f = (\frac{t_c}{\Delta_t} - 1)S_m \qquad 3\text{-}21$$

4. Calculate the fracture hydraulic diffusivity:

$$\eta_f = \frac{10^{[3.23-0.87(s)]} r_w^2}{T_f} \qquad 3\text{-}22$$

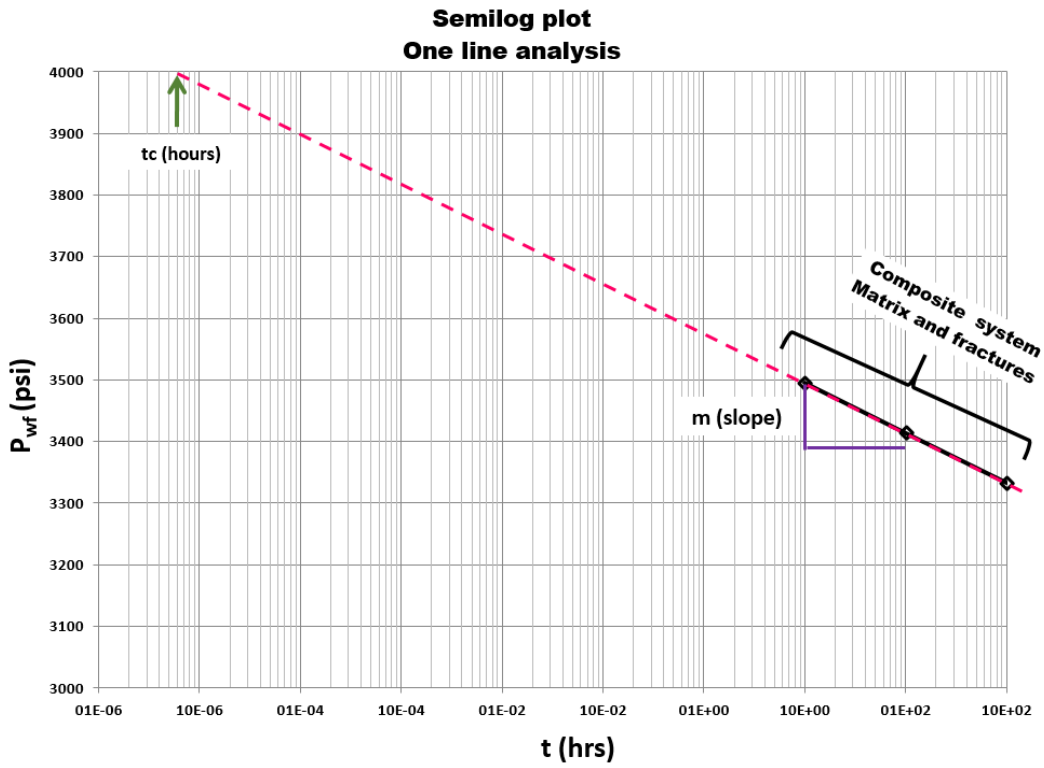

Figure 3-4: Semilog plot (bottom hole pressure vs time); one straight line (NFR Class, University of Calgary).

Radius of investigation: This variable was in function for the duration of time of a drawdown or build up test and of the reservoir geological characteristics:

$$r_{inv} = \sqrt{0.00105}\eta_g t \qquad 3\text{-}23$$

where η_g is the time dependent hydraulic diffusivity and t is flow time in hours.

All the equations and methodologies mentioned in this chapter were applied in drawdown and buildup tests, when applicable; $\Delta p = p_{ws} - p_{wf}$, and $\Delta p = p_i - p_{wf}$ for buildup and drawdown tests, respectively.

$$\Delta p = p_{ws} - p_{wf} = \frac{162.6qB}{T_f}\left[\log\left(\frac{\eta_g^t}{r_w^2}\right) - 3.23 + 0.87(s)\right] \qquad 3\text{-}24$$

Chapter Four: **FRACTAL THEORY FOR NATURALLY FRACTURED RESERVOIRS**

4.1 Introduction

Since 1990, Chang and Yortsos (1990), Olarewaju (1996), Beier (1994) and Camacho (2001) have applied fractal models to pressure transient responses of naturally fractured reservoirs without Euclidean geometry, where the main premise is that different scales, poor fracture connectivity and disorderly spatial distribution are present and a fractal fracture network is embedded in an Euclidean matrix (Figure 4-1).The Bourdet derivative technique is the best tool to identify fractal behavior, where the well bore pressure is a power law function of time and the spectral dimension can be calculated. This parameter is a function of two fractal parameters: fractal dimension (d_{mf}) and connectivity index (θ). The pressure transient responses of such models using the Bourdet semi logarithmic derivative on a log log plot are two parallel straight lines with the same slope; the slope value indicates the fractal flow behavior. The following authors analyzed the pressure transient responses in these types of reservoirs: Chang and Yortsos (1990) applied a fractal model to a pressure transient analysis. It defines a system with different scales, poor fracture connectivity and disorderly spatial distribution. Olarewaju (1996) examined the pressure transient response of NFR by using fractal models, but instead of assuming a pseudo steady state transfer function between the matrix and fracture systems, he assumed a transient interporosity flow assumption. Beier (1994) extended the fractal model of Chang and Yortsos to analyze a hydraulically fractured well. He also observed a power law behavior during the linear and radial flow periods. Flamenco and Camacho (2001) based on previous studies analyzed the pseudo steady state matrix to fractal fracture transfer

function, in order to calculate the fractal parameters, such as the connectivity index *(θ)* and fractal dimension *(d_{mf})* [17].

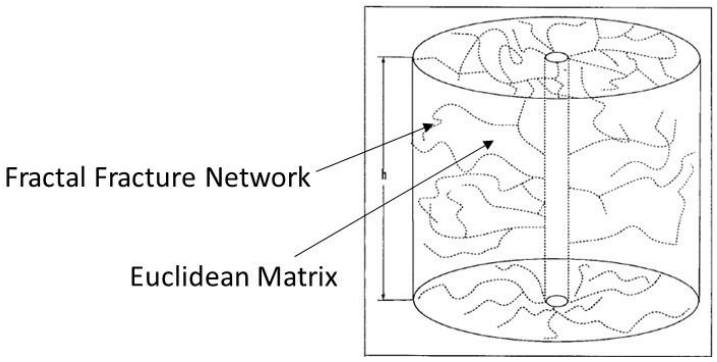

Figure 4-1: Fractal model description by Chang and Yortsos (1990).

4.2 Fractal parameters [1]

Fractals are geometric objects that remain statically invariant upon a change of scale. A basic characteristic of fractal objects is that many of their properties, defined as volume averages over a region of scale *(r)*, are scale dependent and statically vary with a power law behavior.

In order to understand how this power law behavior is applied in a fracture network , it is important to consider the calculation of the fracture density by taking a circle of radius *r* around an arbitrary point, where all the networks are embedded in a dimension (*d = 2*).

Network 4-2a: Corresponding to a single fracture only, the mass of a fracture network (one fracture) increases as $M(r) \alpha r$, while the area (volume) of the circular region increases as $A(r) \alpha r^2$. The fracture density behaves as $\rho(r) \alpha r^{-1}$ (Equation 4-1) with a $d_{mf}=1$ and $d=2$,

where the single fracture is embedded in *d=1*. It is density that would have remained invariant of *r*.

$$\rho\,(r)\;\alpha\; r^{\,dmf-d} \qquad 4\text{-}1$$

where d_{mf} is the mass fractal dimension and *d* is the Euclidean dimension (embedding dimension).

Network 4-2b: Due to its fractal structure, it has a power law behavior but now with a higher fracture density, $1<d_{mf}<2$.

Network 4-2c: Is the more traditional network, which has a constant fracture density with a $d_{mf}=d=2$. This network represents the typical Warren-Root double porosity model.

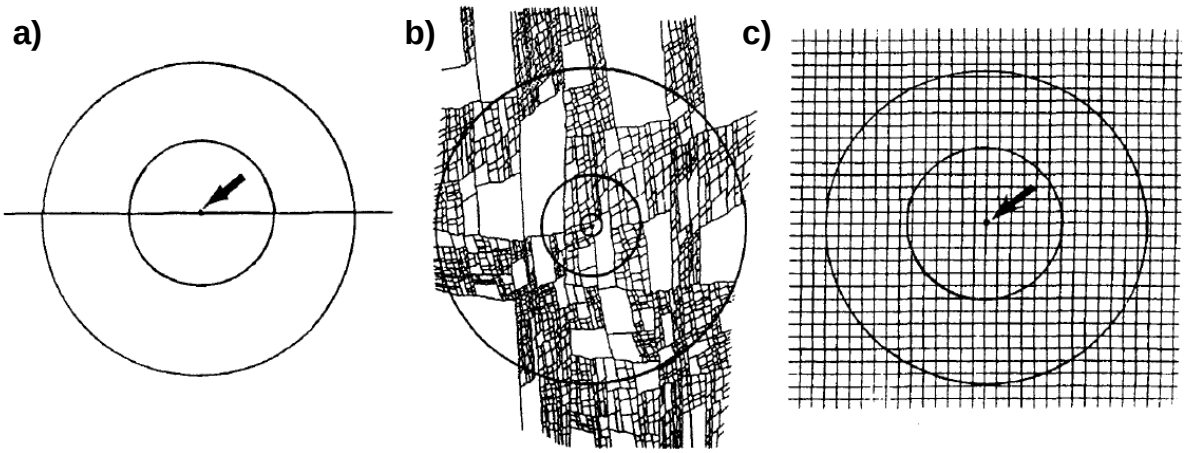

Figure 4-2: Networks in a 2D embedding medium *d*=2. a) d_{mf} =1 (Euclidean),b) 1< d_{mf} <2 (Fractal), and c) d_{mf} =2 (Euclidean) by Chang and Yortsos (1990).

The mass fractal dimension parameter (d_{mf}) gives information related to the fracture density in a porous medium; Figure 4-3 shows three examples of 2D synthetic fractal networks

with different fractal dimensions. As d_{mf} increases the fracture density increases and vice versa.

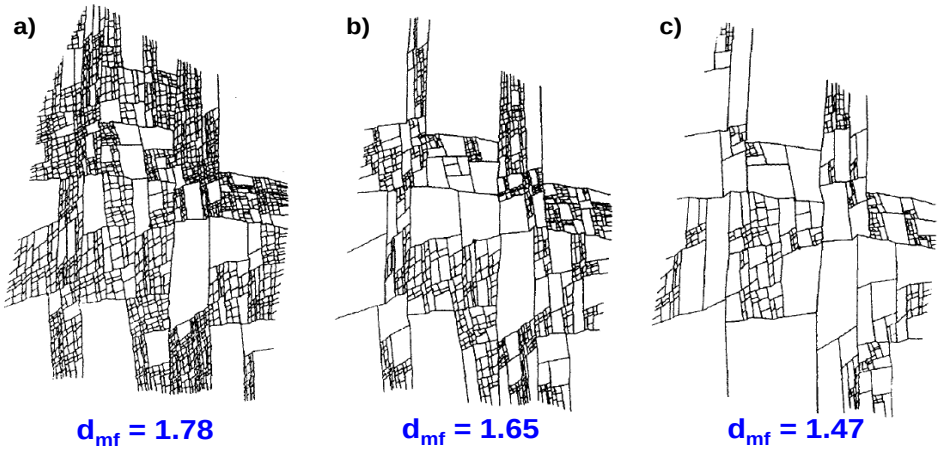

Figure 4-3: Fractal networks in 2D with different fractal dimensions by Chang and Yortsos (1990).

The exponent θ (connectivity index) is related to diffusion or conduction. This parameter is related to the spectral exponent. To understand its meaning, we consider a single particle diffusing from the origin (well) and remember that single phase pressure transient in reservoirs is based on the diffusion phenomenon. In diffusion for fractal objects the average distance of the particle from the origin at time (t) obeys the following equation.

$$< R^2 > \alpha\ t^{\,2/(2+\theta)} \qquad 4\text{-}2$$

When $\theta=0$, the connectivity is high and the diffusion is not obstructed. This behavior applies in cases 4-2a and 4-2c, both with Euclidean geometry. On the other hand, when $\theta>0$, the diffusion in a fractal network is affected due to poor fracture connectivity between fractures. For this reason the connectivity index (θ) is greater than 0, as in case 4-2b.

4.3 Spectral dimension [1]

Chang and Yortsos (1990) proposed a method of modelling pressure transient tests using a generalized diffusivity equation. This method is valid in asymptotic sense (large time) for a well at the origin producing at a constant rate, and the pressure response is in a dimensionless form.

$$p_D(r_D, t_D) = \frac{r_D^{(2+\theta)(1-\delta)}}{\Gamma(\delta)(2+\theta)} \ \Gamma[1-\delta, \frac{r_D^2}{(2+\theta)^2 t_d}] \qquad 4\text{-}3$$

where:

p_D (r_D, t_D) is the dimensionless pressure drop at dimensionless distance r_D and time t_D.

$$\delta = (d_{mf}) / (2+\theta) \qquad 4\text{-}4$$

where:

δ is the spectral dimension.

$\Gamma(x)$ is the gamma function and $\Gamma(x, y)$ is the incomplete gamma function.

For a small value of the argument $(r_D{}^{2+\theta})/(2+\theta)^2 t_D$, which at wellbore occurs after a short time, we may use only the first two terms of the series expansion of $\Gamma(x, y)$ to obtain in dimensional notation, Equation 4-5.

$$p_w(t) = A + B\frac{(2+\theta)^{1-2\delta}}{(1-\delta)\Gamma(\delta)} t^{1-\delta} \qquad 4\text{-}5$$

where: A and B are constants.

Characteristics of the Spectral Dimension.

The spectral dimension δ carries information about a mass fractal dimension and the connectivity index. This parameter is defined by applying the semi logarithmic derivative

technique; by analyzing the pressure transient flow response, the spectral dimension can be calculated. d_{mf} and θ cannot be calculated, and requires additional analysis.

The spectral dimension defines the type of flow behavior based on two cases:

a) $\delta < 1$: $d_{mf} < 2$ (flow behavior intermediate between linear and radial).

b) $\delta > 1$: $d_{mf} > 2$ (flow behavior intermediate between radial and spherical).

Case $\delta < 1$: The bottom hole pressure can be approximated as $p_w(t) \sim Ct^{1-\delta}$.

where:

- *C* is a dimensional constant
- *t* is the dimensional time

No wellbore skin was assumed. The logarithmic pressure derivative behaves as $dp/d\log(t) \sim C(1-\delta)t^{1-\delta}$. These two expressions suggest that the log log plots of pressure and derivative vs time will appear as two straight parallel lines. The pressure derivative vs time in a log log plot will be a straight line, now with a positive slope (Figure 4-4). The spectral dimension is calculated from the following equation.

$$\delta = 1 - m \qquad 4\text{-}6$$

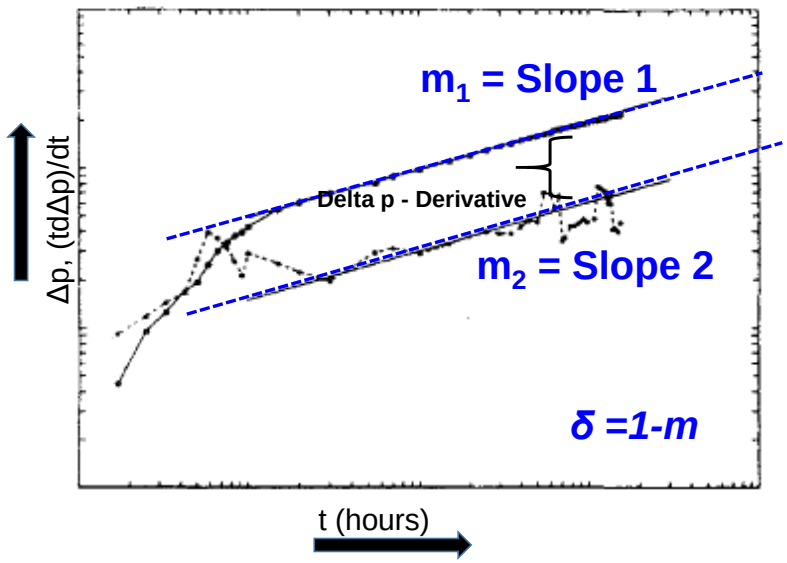

Figure 4-4: Log-log plot, typical fractal behavior when $\delta < 1$

Case $\delta > 1$: This case requires a structure where flow also occurs parallel to a wellbore. A possible scenario is a partially completed well in a thick formation or a well intersecting a few productive fractures. This behavior is very common at early times in many well tests in naturally fractured reservoirs and indicates how the fractures feed directly into the well and require some time before they start to respond as an effective composite system.

The asymptotic behavior for Equation 4-5 is different. The time independent term now dominates at a large time, the time dependent term is negative, and the pressure behaves as $p_w(t) = A - Ct^{1-\delta}$, where A and C are positive. A is the asymptotic pressure at a long time, however, the pressure derivative, given by $dp/d\log(t) = C(1-\delta)\, t^{1-\delta}$, is still a power law function of time.

The pressure derivative vs time in a log log plot will be a straight line, now with a negative slope Figure 4-5.

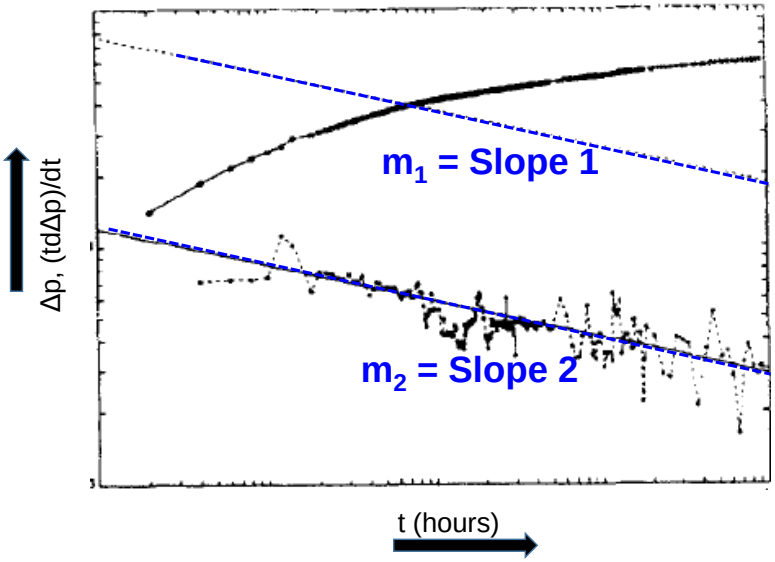

Figure 4-5: Log-log plot, fractal pressure transient behavior corresponding to a well from the Geysers geothermal field.

To calculate the value of the constant *A* from the pressure plot, it is necessary to do the following steps:

Draw a line above and parallel to the pressure derivative curve, separated by a distance *log (1/ (δ-1))*, as shown in Figure 4-5; this line represents the term $C_t^{1-\delta}$ *or A-* p_w *(t)* at the point where this line intersects the original pressure curve. The corresponding pressure value must be equal to *A/2*, from which the constant *A* can be calculated.

Validation of a fractal behavior.

In order to validate a fractal behavior, the semi logarithmic derivative technique is applied. The following characteristics must be considered:

- Consider the storage and production time effects before a buildup test, mainly because both tend to mask the power law behavior (fractal geometry).
- The slopes measured from a buildup test in a log log plot of both pressure increment and semi logarithmic derivative are the same. This behavior must remain more than ½ cycle in the log log plot in order to be significant.
- Compare the value obtained from the difference between pressure and the pressure derivative data at a defined time from a log log plot Figure 4-4. vs the difference calculated from the equation log (1/m), where *m* is the value of the slope; both values have to be similar.

4.4 Calculation of permeability *(k_w)* and skin factor (s) for fractal reservoirs

The calculations of the permeability *(k_w)* and the skin factor *(s)* are very important because they indicate if a reservoir requires activities such as: minor or major workovers, stimulations, and fracturing, in order to increase the oil and gas production of the oilfield. To compute the permeability and skin factor for fractal reservoirs, the fractal parameters such as fractal dimension (d_{mf}) and connectivity index (θ) must have to be considered. This is the reason for developing a methodology to compute them. The following methodology was based on paper SPE 71591[20], where the skin factor was considered based on Equation 4-7 for an infinite fractal reservoir without matrix participation.

4.4.1 Permeability (k_w) equation for fractal reservoirs

Equation 4-7 is given in dimensionless variables and the behavior of this equation depends on whether $v > 0$ or $v < 0$, where v is given by Equation 4-10. The first case considers

d_{mf}<2, resulting in a log log plot of pressure and pressure derivative versus time in two parallel straight lines with positive slope. The second case considers d_{mf} >2, resulting in a log log plot of pressure and pressure derivative versus time in one parallel straight line with a negative slope v. [20]

$$\boldsymbol{p_{wD}\,(t_D)}=\frac{\mathbf{1}}{-\boldsymbol{v}\,(\mathbf{2}+\boldsymbol{\theta})}+\ \frac{(\mathbf{2}+\boldsymbol{\theta})^{\mathbf{2}\boldsymbol{v}-\mathbf{1}}}{\boldsymbol{v}\Gamma\,(\mathbf{1}-\boldsymbol{v})}\,\boldsymbol{t_D^v}+\boldsymbol{s}$$

4-7

where:

$$\boldsymbol{t_D}=\frac{\boldsymbol{k_w(t)}}{\boldsymbol{\phi_w}\mu\boldsymbol{r_w^{2+\theta}C_t}}$$ 4-8

$$\boldsymbol{p_D}=\frac{\boldsymbol{k_w(h)(\Delta p)}}{\boldsymbol{q}\mu\boldsymbol{B}}$$ 4-9

$$\boldsymbol{v}=\frac{\mathbf{1}-ß}{\boldsymbol{\theta}+\mathbf{2}}$$ 4-10

$$ß=\boldsymbol{d_{mf}}-\boldsymbol{\theta}-\mathbf{1}$$ 4-11

d_{mf}: Fractal dimension

θ: connectivity index

Γ: gamma function

s: skin factor

k_w: permeability (md)

t: time (hours)

Δp: pressure drop (psi)

ϕ_w: Porosity (fraction), from core analysis

μ: viscosity (cp)

r_w: well radius (ft)

Ct: Total compressibility (psi^{-1})

B: oil formation factor (RB/STB)

q: oil flow rate (STB/D)

h: formation thickness (ft)

Substituting Equations 4-8 and 4-9 in Equation 4-7, Equation 4-12 was obtained:

$$\frac{k_w h\Delta p}{q\mu B} = \frac{1}{-v(2+\theta)} + \frac{(2+\theta)^{2v-1}}{v\Gamma(1-v)} \left(\frac{k_w(t)}{\phi_w \mu r w^{2+\theta} Ct}\right)^{v} + s \qquad 4\text{-}12$$

From Equation 4-12; Δp for fractal reservoirs was defined by the following equation:

$$\Delta p = \frac{q\mu B}{k_w h}\left(\frac{1}{-v(2+\theta)}\right) + \frac{q\mu B}{k_w h}\left(\frac{(2+\theta)^{2v-1}}{v\Gamma(1-v)}\right)\left(\frac{k_w}{\phi_w \mu r w^{2+\theta} Ct}\right)^{v} t^{v} + \frac{q\mu B}{k_w h} s \qquad 4\text{-}13$$

From Equation 4-13, the slope is defined by the following equations.

$$m = \frac{q\mu B}{h}\left(\frac{(2+\theta)^{2v-1}}{v\Gamma(1-v)}\right)\left(\frac{k_w}{\phi_w \mu r w^{2+\theta} Ct}\right)^{v} \qquad 4\text{-}14$$

$$m = \frac{q\mu B}{h}\left(\frac{(2+\theta)^{2v-1}}{v\Gamma(1-v)}\right)\frac{k_w^{v}}{k_w}\frac{1}{(\phi_w \mu r w^{2+\theta} Ct)^{v}} \qquad 4\text{-}15$$

$$m = \frac{q\mu B}{h}\left(\frac{(2+\theta)^{2v-1}}{v\Gamma(1-v)}\right)\left(\frac{1}{(\phi_w \mu r w^{2+\theta} Ct)^{v}}\right)k_w^{v-1} \qquad 4\text{-}16$$

Finally from Equation 4-16, the proposed equation to compute k_w was defined:

$$k_w^{v-1} = \frac{m}{\frac{q\mu B}{h}\left(\frac{(2+\theta)^{2v-1}}{v\Gamma(1-v)}\right)\left(\frac{1}{(\phi_w \mu r_w^{2+\theta} C_t)^{v}}\right)} \qquad 4\text{-}17$$

4.4.2 Methodology to define the slope from diagnostic Cartesian plot

From Equation 4-17 the permeability can be obtained; however, in order to apply it, the slope (m) must be known. For this the following procedure was proposed:

- From buildup test data calculate Δp (psi)
- From Equation 4-10, v is calculated
- From buildup test data calculate the $time^v$;
- Build a Cartesian plot *(Δp vs $time^v$)* from the buildup test, Figure 4-6: Δp *vs* $\boldsymbol{time^v}$, Cartesian plot.
- The straight line identified in the Cartesian plot is the slope (m) in $\frac{psi}{hour^v}$.

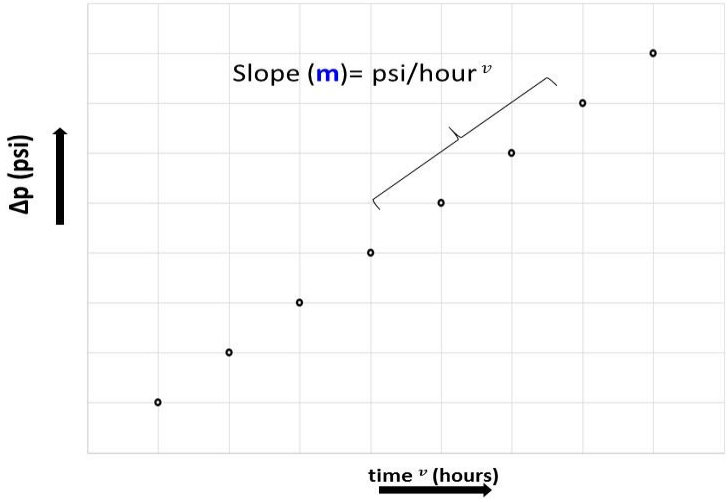

Figure 4-6: Δp vs $\boldsymbol{time^v}$, Cartesian plot.

4.4.3 Skin factor (s) equation for fractal reservoirs

In order to compute the skin factor, Equation 4-13 was considered, leading to Equation 4-18.

$$\Delta p = (m)\,(t) + \frac{q\mu B}{k_w h}\left(\frac{1}{-v(2+\theta)}\right) + \frac{q\mu B}{k_w h}s \qquad 4\text{-}18$$

Then intercept (b) was defined by the following equation:

$$b = \frac{q\mu B}{kwh}\left(\frac{1}{-v(2+\theta)} + s\right) \qquad 4\text{-}19$$

where $b = \Delta p$ *(psi);* (Figure 4-7)

Finally from Equation 4-19, the following equation was defined:

$$s = \frac{bhk_w}{141.2\ q\mu B} - \left(\frac{1}{-v(2+\theta)}\right) \qquad 4\text{-}20$$

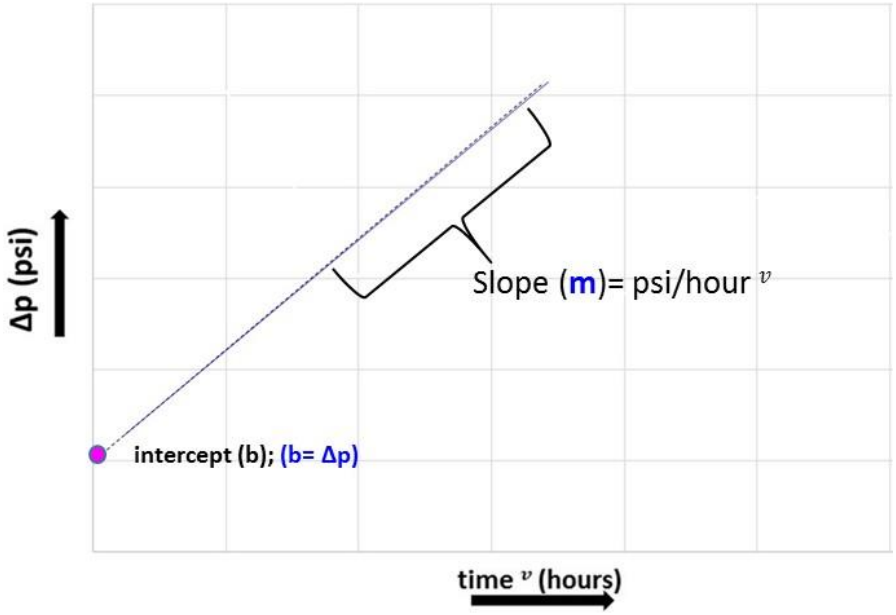

Figure 4-7: Δp vs $\boldsymbol{time^{v}}$, Cartesian plot.

Chapter Five: **DETERMINATION OF FRACTAL PARAMETERS USING STATISTICAL ANALYSIS**

5.1 Introduction [22]

Statistical fractals are objects that have some statistical properties, in order to explain why the properties are important for a reservoir description. First, it is necessary to mention some basic statistical assumptions covered in the section named ensembles and some basic statistical measures mentioned in the section named univariant measures. Second, in the section multivariant measures some complex statistical measures are noted. Finally, the Fractional Gaussian noise (fGn) and Fractional Brownian motion (fBm) fractal models are explained in terms of statistical measures.

5.1.1 Ensembles

An ensemble is a collection of similarly prepared tests. This concept can be applied to analyze reservoir properties such as depositional units (layers deposited in a similar depositional environment). The ensembles are stationary and ergodic, both of which are related to time average and ensemble average respectively. The stationary ensemble is one whose ensemble and time averages are the same. It means that the ensemble average must be independent of time and the time average independent of the trace. An ergodic ensemble must be stationary, but this ensemble is not an ergodic. It means that an ergodic ensemble is one whose ensemble and spatial averages are the same. Stationary and ergodicity are assumptions that allow us to predict behaviors, for instance, the prediction related to the porosity property from a new formation when a well is expected to be drilled. The lack of

stationary and ergodicity does not mean that we cannot make statistical predictions; it does mean that we cannot use statistical tools that trust in this assumption.

5.1.2 Univariant Ensembles

Univariant statistical measures describe data without order. This is called *bucket statistics.* This describes that the data is dumped into a bucket and then drawn out in any order. Most of the statistical measures are related to a classification such as mean, standard deviation, histograms and Dystra Parson's coefficient.

When applying this statistical analysis in reservoir property distributions, typically the values of these properties from zones or regions are based on geologic units. The data from each zone is dumped in a bucket and one or all of the univariant measures described above are calculated.

Univariant statistics do not provide enough information about these reservoir properties such as porosity and permeability for fluid flow simulations, because the univariant statistics cannot describe all the heterogeneity. This is important in predicting the dynamic behavior of the reservoirs.

5.1.3 Multivariant measures

The multivariant measures are more diverse than the univariant measures such the following multivariant methods:

- Covariance or auto covariance: describes the amount of correlation among sample values. It is a function of the distance between samples and requires many points

for accurate answers. The covariance is used to analyze the time sequences in statistical physics.

- Variogram or semi variogram: measures how fast a sample sequence varies. There is no variation between the values of a point itself, as lags increase. The variogram increases because it is related to an effect called a nugget in geostatistics analysis and is used in geostatistics analysis.
- Spectral analysis (Fourier transforms): is a statistical measure based on the Fourier transform of the original data. The Fourier transform turns a sequence of data into a set of sine and cosine curves, both of which reproduce the original tendency. The spectral analysis is used in electric engineering, seismic processing and image analysis.
- Rescaled range analysis (R/S): is focused on how a sequence varies as a lag increases. The range is a measure of the cumulative variation of a sequence. This range (R) is divided by

  the standard deviation (S) of each range (R/S). Based on a log log plot (R/S vs the number of ranges), the slope calculated is called the Hurst exponent (H). This analysis is commonly used in fractal analysis.

In **Figure 5-1**some crossplot examples of each method are showed.

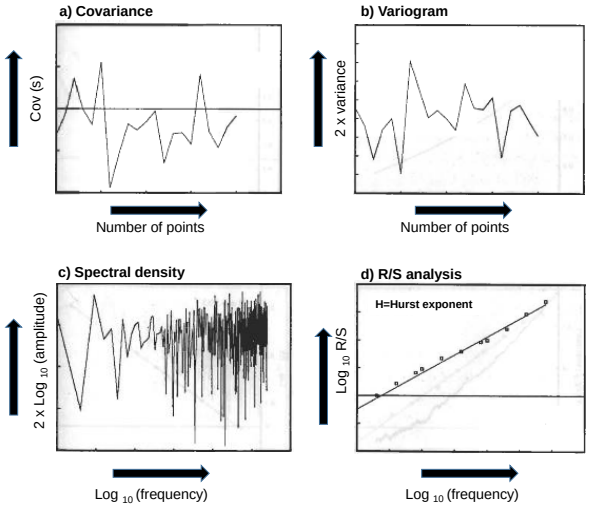

Figure 5-1:Example plots of multivariant methods: a) Covariance method, b) Variogram method, c) Spectral density method and d)R/S analysis.

5.1.4 Fractal models

In this section, the multivariant statistical methods can be applied to the fractional Gaussian noise (fGn), and the fractional Brownian motion (fBm) traces are sequences with a fractal character. They are used to describe reservoir property distributions, based on three parameters: the mean, the standard deviation, and the slope calculated from a spectral density plot. The mean and standard deviation of fGn and fBm can be calculated from any determined value. The histogram of fGn is Gaussian, the histogram of fBm is box shaped, and fGn and fBm have spectral densities (S) that scale with angular frequency (ω).

$$S \alpha \omega^{\beta} \ldots \quad 5\text{-}1$$

The value of *ß* for fGn is between +1 and -1; for fBm it is between -1 and -3. For fGn the slope of the spectral density is related to the slope calculated form R/S analysis plot (H=Hurst exponent).

$$S \alpha \omega^{\beta} \ldots \quad 5\text{-}2$$

For fBm, this relationship is:

$$\beta = -(2H + 1) \qquad 5\text{-}3$$

In Figure 5-2 fGn and fBm traces examples are shown. The fGn is nosier than fBm as *ß* decreases. This analysis can be more accurate with the application of the multivariant statistical plots.

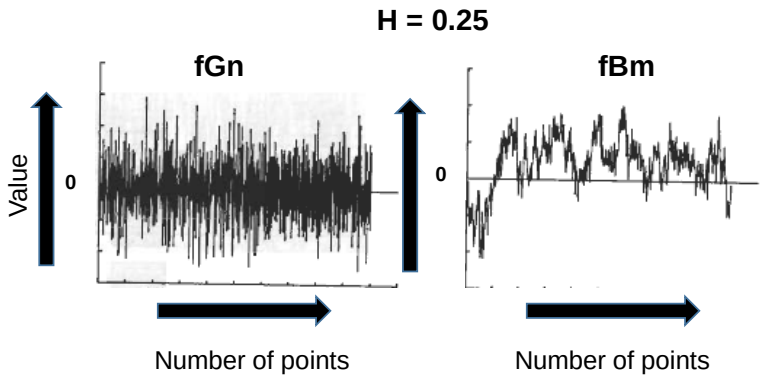

Figure 5-2: Examples of fGn and fBm data sets for a defined Hurst value of 0.25.

5.2 Rescaled range analysis (R/S) based on wire line logs

5.2.1 Introduction

As explained in Chapter 4, by only analyzing the pressure transient response from a well test, it is possible to identify a spectral dimension *(δ)*, which carries information about the mass fractal dimension and connectivity index**.** For this reason, an additional methodology must be applied to estimate the mass fractal dimension. The rescaled range analysis (R/S) can be used in order to calculate d_{mf} based on the value of the Hurst exponent. The fractal theory is related to complex natural objects, which cannot be represented by an Euclidean space. The best way is to reproduce the complex geological phenomena by applying the

fractal theory. In this case, the mass fractal dimension can be obtained by the response of wire line logs, which represent a very small section of the whole reservoir, but can be applied at larger scale to analyze reservoir features between wells. Many authors have applied the fractal theory to analyze geological data; for instance; Hewett (1986) discussed fractal distributions of reservoirs heterogeneity, and concluded that: *"the self-similar statistics of random fractals provide a good model for the spatial structure of the reservoir property distribution"* [22]. Matthews et al. (1989) used a fractal method for fluid –flow prediction in a channel-sands reservoir, and decided that the results were better than those from traditional approaches [44]. Crane and Tubman (1990) applied fractals to both vertical and horizontal well logs in order to examine the spatial variability of reservoir porosity, and discovered similar fractal dimensions. They also used Fourier transform techniques to generate fractal reservoir cases. Scholz and Barton (1991) found that the size distributions of oil accumulations obey a fractal size distribution.

5.2.2 Calculation of Hurst exponent (H)

A R/S analysis was invented by Harold Ewin Hurst (1880-1978) by quantifying the long term discharge variations of the River Nile (1965), defining the Hurst exponent which is used as a measure of long term memory of time series in a fractal analysis. The Hurst exponent is denoted by (*H*), which is related to the fractal dimension. For a geological analysis where no theoretic fractal dimension is available, it is normally estimated from known samples by different approaches, such as a spectral density analysis and rescaled range (R/S). Hewett (1986) observed that the scaling relations of the spatial correlation in

fractal distributions can be determined from the asymptotic behavior of the rescaled range (R/S) in conjunction with other tools of geostatistics[22].

Later, the method was proved resulting in an efficient technique for analyzing one dimensional fractal variables (Mandelbrot and Van Ness, 1968; Mandelbrot and Wallis, 1968, 1969).

Mandelbrot and Wallis (1969) and Feder (1988) established Equations 5-4, 5-5 and 5-6 to obtain the fractal dimension of a given sequence [16]. For a determined one dimensional process, *Z (t)* corresponds to the wire line log curve and the partial sample sequential range *R (t, n) of Z (t).*

$$R(t,n) = \max_{0<u<n}\{\sum_{i=1}^{u} Z(t+i) - (\frac{u}{n})\sum_{j=1}^{n} Z(t+j)\} - \min_{0<u<n}\{\sum_{i=1}^{u} Z(t+i - (\frac{u}{n})\sum_{j=1}^{n} Z(t+j)\} \quad 5\text{-}4$$

where u is a discrete integer –value a sample number corresponding to depth for wire line log readings (equivalent to time in a time series application); *n* is the time-span considered indicating the sequence interval or the number of data points (*n+1*) of the calculated range; and *t* is the start point (first sample number) of the samples used for calculation. The ranges of different processes, *R (t, n)* must be compared; the sample variance S^2 is defined in Equation 5-5 [43].

$$S^2 = 1/n\sum_{i=1}^{n} Z^2(t+i) - [\frac{1}{n}\sum_{j=1}^{n} z(t+j)]^{\ 2} \quad 5\text{-}5$$

A process is considered to be fractal when the log log plot of R/S versus the number of ranges shows an aligned straight trend line. The slope of this line is called the Hurst exponent (*H*), (Figure 5-3) which is related to the local fractal dimension d_{mf} (Equation 5-6).

d_{mf} =2-H 5-6

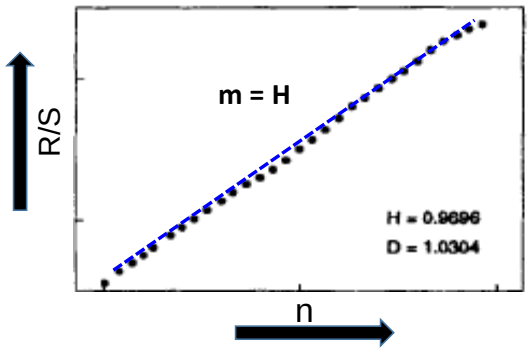

Figure 5-3: Example of R/S analysis, log log plot

5.2.3 Consideration to calculate the fractal dimension (d_{mf})

Data from wire line logs must correspond to reservoir section. The logs more suitable for this analysis can be sonic, gamma ray and neutron logs, because they give us information about lithology. If the reservoir has several formations, it is important to do the analysis for each formation separately.

According to Mandelbrot and Wallis (1969) and Feder (1988), the sample set must be greater than 1000 points in order to get a reliable Hurst exponent ($H<1$) and get a reliable analysis. On the other hand if H is greater than 1, it means that there are not enough data sets, resulting in an unreliable value of H [22, 43].

5.2.4 Methodology to calculate the fractal dimension (d_{mf})

The following proposed methology explains step by step how to obtain the fractal dimension from the Hurst exponent.

a) Estimation of H:

1. Select the petrophysical data to analyze from well logs responses.
2. Define the range of data sets because the rescaled range is based on multiple ranges of data.
3. Calculate the mean for each range and for the total data.

$$\text{mean}_s = m_s = \frac{1}{n}\sum_{i=1}^{n} X_i \quad \text{5-7}$$

where:

s = series of data

n = the size of the range for which the mean is calculated

X = the value of one element in the range selected

4. Create a series of deviations for each range. This creates another series of data using the mean of each range.

$$Y_t = X_t - m; for\ t = 1,2..,n \ldots \quad \text{5-8}$$

where:

Y = the new time series adjusted for deviations from the mean

X = the value of one element in the range selected

m = the mean for the range calculated previously.

5. Create a series, considering the total of deviations from the mean in order to get a series of deviations from the mean for each range.

$$y = \sum_{i=1}^{t} Y_t \quad \text{5-9}$$

where:

y = total of the deviations from the mean for each series

Y = the series adjusted for deviations from the mean

6. Calculate the widest difference in the series of deviations. Find both the maximum and minimum values in the series of deviations for each range. Take the difference between the maximum and minimum in order to calculate the widest difference.

$$R_t = \max(Y_1, Y_2, \dots, Y_t; -\min(Y_1, Y_2, \dots, Y_t) \text{ for } t = 1,2, \dots, n \quad 5\text{-}10$$

where:

R = the widest spread in each range

Y = the value of one element in the "deviations from the mean" range

7. Calculate the standard deviation (*S*) for each range. There will be a standard deviation calculation for each range and for the total set of data.

$$\sigma = \sqrt{\frac{1}{t}\sum_{i=1}^{t}(X_i - m)^2} \quad 5\text{-}11 \text{ ; for } t=1, 2 \dots n$$

8. Calculate the rescaled range (R/S) for each one. This step creates a new measure for each range in the time series that shows how wide the range is measured in standard deviations by dividing the value obtained in step 6 (*R*) by the standard deviation for each range (*S*) in step 7.
9. Build a table with the numbers of ranges defined and the values of *R/S* calculated for each range.
10. Plot the *R/S* vs *n* (number or ranges) in a log log plot. The slope calculated from this plot is the Hurst exponent.
11. The mass fractal dimension (d_{mf}) is calculated by Equation 5-6 and connectivity index (θ) by Equation 4-4.

Through the analysis of the pressure transient response, it is possible to define the spectral dimension (δ). Based on the proposed methology of *R/S* analysis, the mass fractal dimension (d_{mf}) and connectivity index (θ) can be calculated. This results in better understanding of the dynamic behavior of the reservoir, by knowing the fracture density and the connectivity between fractures, which affects the hydrocarbon recovery factor.

Chapter Six: **INFLUENCE OF FRACTAL PARAMETERS ON PRODUCTION DECLINE**

6.1 Introduction

In order to evaluate the production performance of these types of reservoirs, it is necessary to take into account the effect of the fractal parameters (d_{mf} and θ) on production decline behavior. This chapter investigates their effect, based on the analytical solutions defined in Reference 9, Camacho et al. (2008).

6.2 Rate and cumulative production evaluation for infinite NFR

The analytical solution considered in this chapter is based on long-time approximations, when the matrix does not participate. The basis of this is from the diffusion equations developed by Chang and Yortsos (1990) and O'Shaughnessy and Procaccia (1985).

The following equations[32] were used in order to generate the rate decline curves (q_{wD}) and the cumulative production curves (N_{pD}), respectively.

$$q_{wD}\,(t_D) = \frac{(2+\theta)^{1-2v}}{\Gamma(v)}\, t_D^{-v} \qquad 6\text{-}1$$

$$N_{pD}\,(t_D) = \frac{(2+\theta)^{1-2v}\,\Gamma(1-v)}{\Gamma(v)\,\Gamma\,(2-v)}\, t_D^{1-v} \qquad 6\text{-}2$$

where t_D and v were defined by Equations 4-8 and 4-10 respectively.

The main premises considered in this analysis were:

- The parameter d_{mf} is fixed at 1.65
- Four fractal cases were defined with different values of θ.

- One Euclidean case was considered, where $\theta=0$.

Figure 6-1 presents rate solutions for one Euclidean case and four fractal cases, with their corresponding long –time approximations. Results show a considerable difference for late times between the Euclidean and fractal cases. As expected, the flow rates from the fractal cases are smaller than that from the Euclidean case, in which the diffusion is faster because the fracture density is uniform and all the fractures are connected.

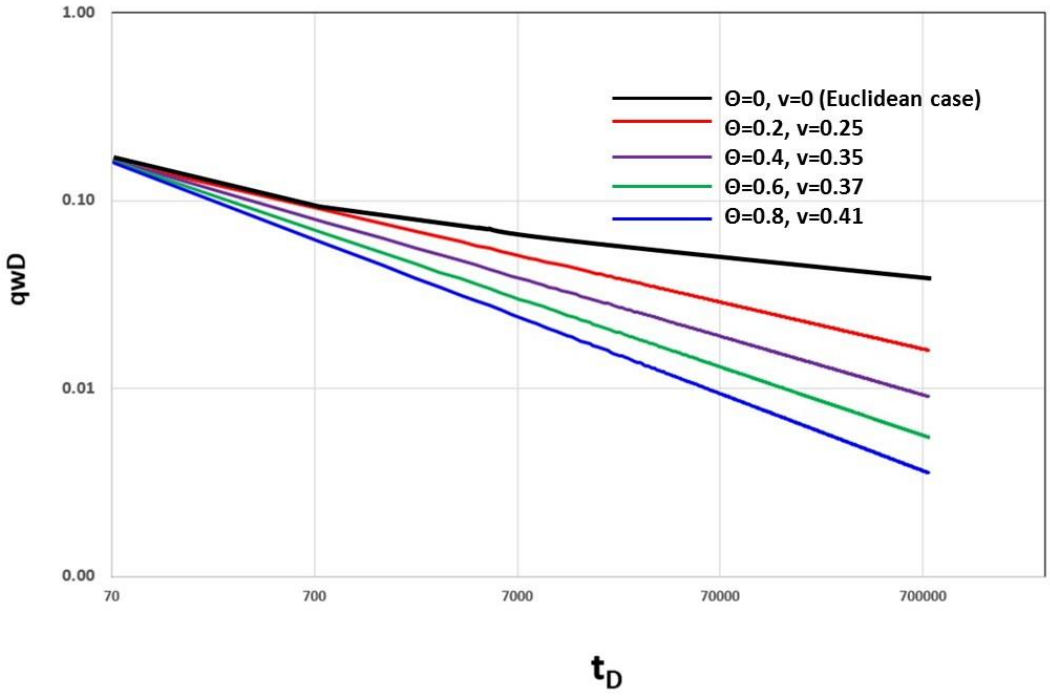

Figure 6-1: Rate (q_{wD}) behavior for fractal and Euclidean reservoirs without matrix participation (long time approximation), log log plot.

Figure 6-2 presents the cumulative production based on Equation 59. These correspond to the rates response presented in Figure 6-1. As expected, the cumulative production (N_{pD}) from the fractal cases is smaller than N_{pD} from the Euclidean case, because in the fractal cases the connectivity index (θ) is greater than 0. This means that oil is produced from finite connected clusters only. Thus, it is important to consider these results in a development strategy for fractal reservoirs in order to achieve realistic and non-optimistic forecasts.

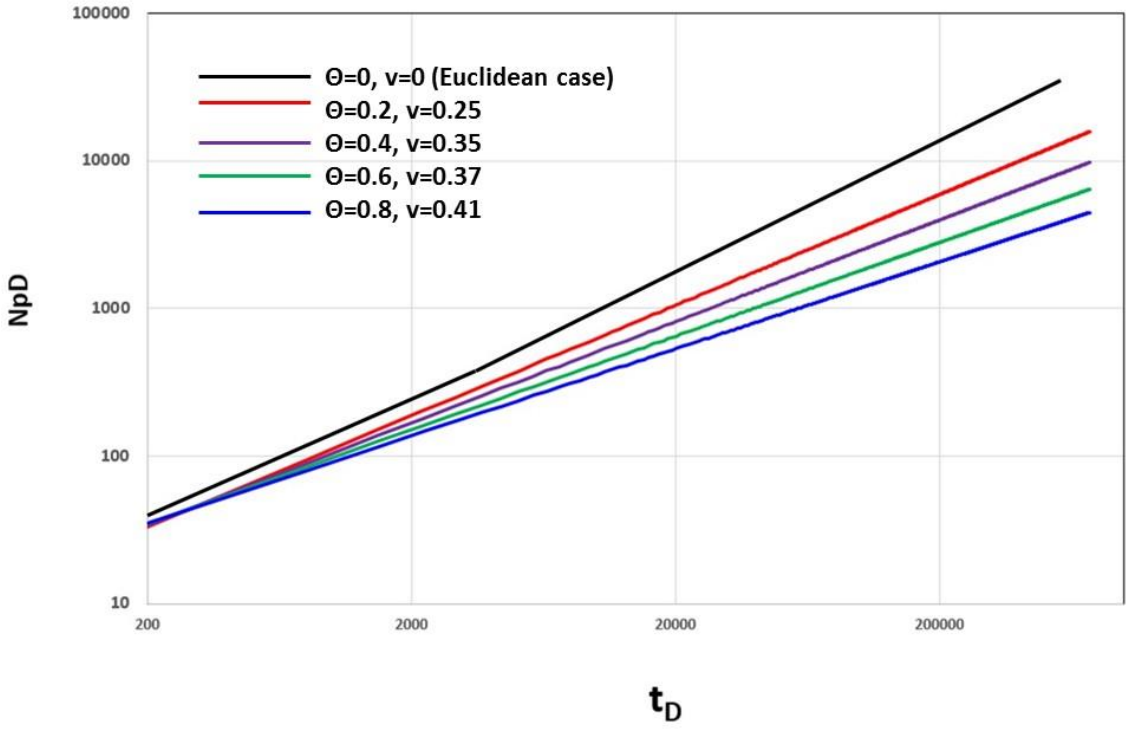

Figure 6-2: Cumulative production (N_{pD}) behavior for fractal and euclidean reservoirs without matrix participation (long time approximation), log log plot.

Chapter Seven: **FIELD CASES**

7.1 Introduction

The idea of this research started in 2013, when two buildup tests from NFRs of the southwest of Mexico, showed a possible fractal behavior in a log log plot of pressure and pressure derivative versus time. The necessity to establish a methodology in order to analyze this type of behavior was identified. These two cases were analyzed using the methodology explained previously: first, the validation of a fractal behavior; second, obtaining the fractal parameters; finally, identifying how these parameters influence the rate flow production of the field.

7.2 General considerations

Well pressure transient tests are very important in the different stages of the oilfield life. First, they give basic reservoir information that allow us to define the initial development strategy of the oilfield based on a reservoir simulation model. Second, based on this information, they propose activities in order to maintain or increase the hydrocarbon production of the oilfield. The following general criteria is based on my experience as a reservoir engineer. The objective is to mention the basic considerations in order to get a reliable well test data set, and then achieve the objective of the proposed well test.

Defining the objective: It is important to define the objective of a well test. What information is necessary to know about the reservoir, taking in consideration of the geologic characteristics of the field. If the well test is for a new area, the dynamic behavior

of neighbour reservoirs must be considered. Fluid samples for PVT analysis, and the quantification of oil and gas production must be considered in the design of the well test.

Defining the time duration for buildup tests: The buildup tests have been considered a problem for the managers of the oil companies, because the well must be shut down and the hydrocarbon production declined. For this reason, it is very important to define the correct time for the buildup test. In order to achieve the objective of the test, the design of the well test must be based on the simulation of each flow regime expected. It is important to review the well tests from neighbour wells because they give us an indication of the type of a flow regime expected in the new reservoir. Based on the geologic characteristics of the area in study and the information of the neighbour wells, the simulation is developed. We consider the optimistic, the realistic, and the pessimist cases, based on the permeability and the skin factor expected. This is very useful in order to define the time of any build up test.

Supervision of the well test on the field: This part of any well test is very important, because we must ensure that all the different disciplines involved in the well test know the objective and the reason to follow the program of the test. The events that happen on the rig during the well test are important and each event must be documented and considered in the analysis report. Most of the bottom hole pressure data is in real time; this is very useful because the analysis of the well is in real time, saving money and time for the oil companies.

Bottom hole pressure analysis: From buildup tests the static bottom hole pressure (P_{ws}) is obtained. P_{ws} gives us information about the current dynamic status of the reservoir. It is important to calculate the P_{ws} to the DATUM (the reference point in the reservoir), which allows us to compare the different P_{ws} taken at different times, and then analyze the pressure declination of the field. From drawdown tests, the flowing bottom hole pressure (P_{wf}) at shut-in is obtained. The P_{wf} gives us information about the current dynamic behavior according to the choke diameter. This is important because based on the productivity index obtained from the nodal analysis and the water cut (%) production identified in the well test, these parameters are going to define the ideal choke in order to start the exploitation of the well.

7.3 Methodology to analyze NFR with fractal geometry

Before analyzing any buildup test in a log log plot of pressure and pressure derivative versus time, it is important to consider the storage and production time effects. These may hide the flow regime related to the behavior of the reservoir. For infinite NFR with fractal geometry and without matrix participation the following proposed methology was applied in two field cases:

- Validate the fractal behavior by applying the semi logarithmic derivative technique based on the criteria explained in Chapter 4.
- Calculate the fractal parameters (d_{mf} and θ) based on the criteria explained in Chapter 5.
- Evaluate the effect of the fractal parameters on production decline

7.4 Field case (reservoir S)

A combined analysis of well testing and production data analysis for a well producing in a field called S, located in the southwest region of Mexico is presented in this chapter to explain the methodology proposed in this thesis.

The field S is a black oil reservoir, which includes an average depth of 3,600 meters, complex NFR. The formation was deposited during the Upper Cretaceous. Detailed geological data has defined an average porosity of 9%. Recent well tests and well-logging studies have estimated an average permeability values of 9 md, for those wells which have Euclidean geometry. The field S has 9 oil producer wells, 3 wells produced from the formation Maastrichtian Upper Cretaceous, and 6 wells produced from the Maastrichtian Upper Cretaceous (Figure 7-1). The matrix in this field is compact, and does not participate in the hydrocarbon production, and therefore, a single porosity analysis was applied. The analysis of this research is based on the wells from the Campaniano Upper Cretaceous, only one well (S-316) showed fractal behavior and the other 5 wells showed Euclidean geometry.

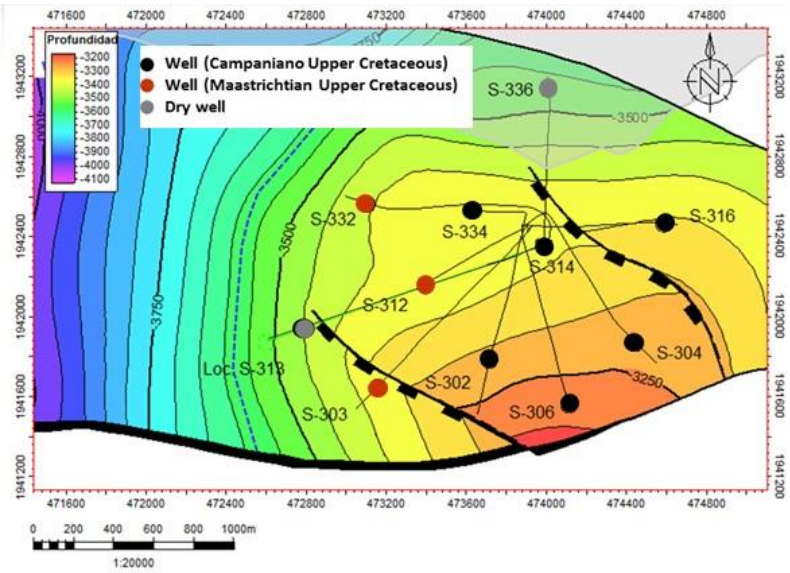

Figure 7-1: Field S (contour map from the formation Upper Cretaceous).

Only four wells have buildup tests (S-302, S-304, S-314, and S-316). These test were analyzed using the semi logarithmic derivative technique (Figure 7-2). The results obtained from the wells with Euclidean geometry are shown in Table 7-1.

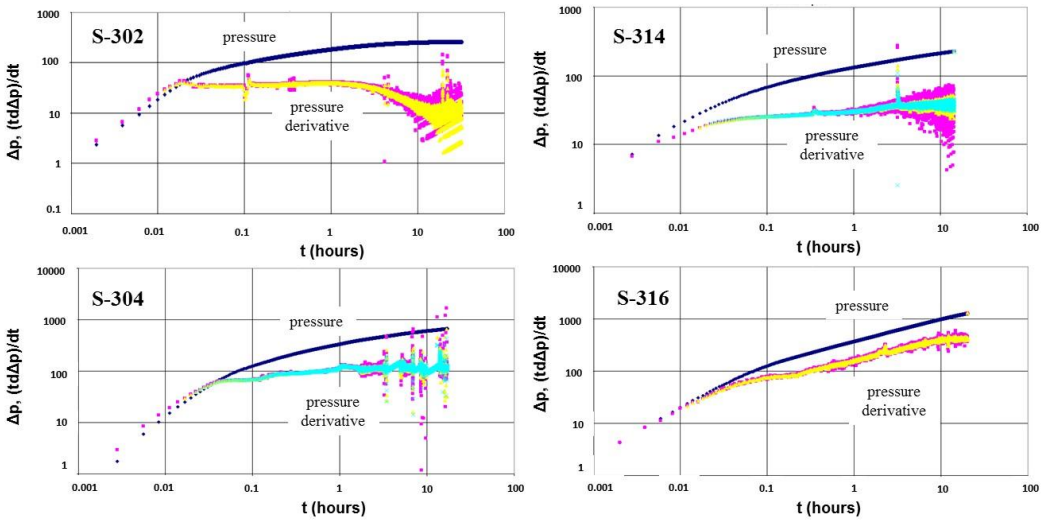

Figure 7-2: Log log plots of pressure and pressure derivative versus time. (Well from Field S- Campaniano Upper Cretaceous).

Table 7-1: Well tests analysis results from wells with Euclidean geometry.

Well	*K* (md)	*kh* (md/ft)	*s* (skin factor)	Model
S-302	17.6	4044	-3.7	Radial homogeneous
S-304	4.6	921	0.05	
S-314	19.8	9422	-1.6	

7.4.1 Well S-316

Validation of fractal behavior: According to the methodology proposed, the first step was to identify the fractal behavior. Table 7-2 shows the input data for well S-316.

Table 7-2: Input data, well S-316

Well	**S-316**	
h	650	ft
Ct	4.5 exp-5	PSI $^{-1}$
Oil rate	856	stb/d
rw	0.27	ft
API	30	
μ	0.8	cp
Bo	1.6	m^3/m^3

Production time before build up test	320	hours

The semi logarithmic derivative technique was applied in order to identify the fractal behavior (**Figure 7-3**). First, it is important to identify the period of time in the buildup test without production effects. For this well the production time before the buildup test was 320 hours. This means that only the first 32 hours from the buildup test are a reliable reservoir response, without production time effects. Second, the validation of the fractal behavior is based on the slopes measured in the log log plot of pressure and pressure derivative versus time (Figure 7-3). Both of these slopes must be the same. This behavior must remain for more than at least ½ cycle in the log log plot. Third, we compare the difference between pressure and pressure derivative at defined times from the log log plot vs the value calculated from the equation: (*1/m*). Both of these must be similar (Table 7-3).

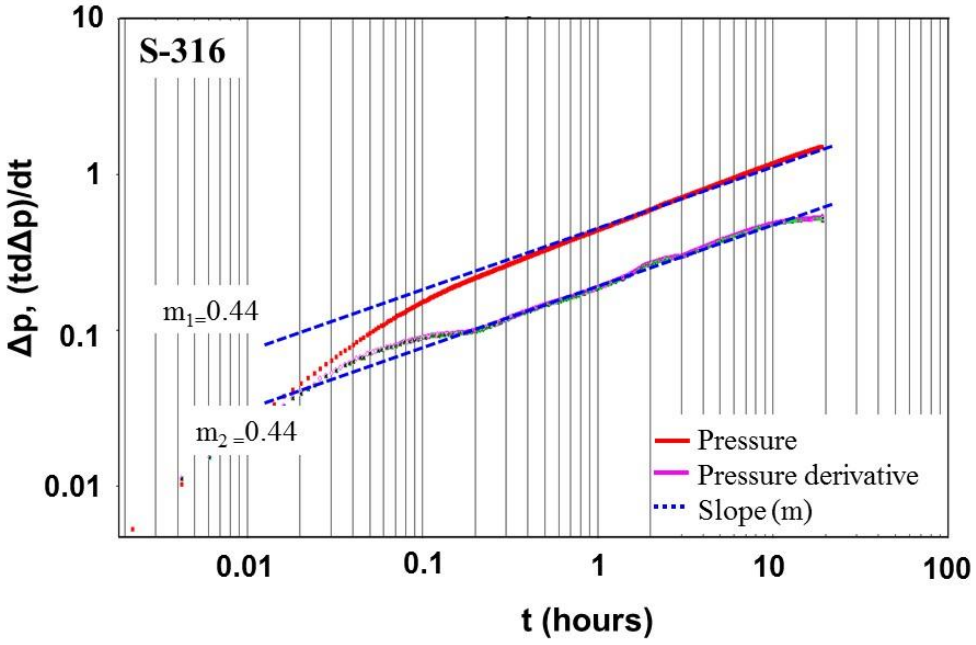

Figure 7-3: Log log plot of pressure and pressure derivative versus time. (Well S-316).

Table 7-3: Results (validation of fractal behavior)

m_1	0.46
m_2	0.46
Log (1/m)	0.34
pressure - pressure derivative @ 1 hour	0.33
Conclusion	**Fractal geometry**

Determination of fractal parameters: Once the fractal behavior was validated, the second step was to calculate the fractal parameters: spectral dimension (δ), fractal dimension (d_{mf}) and the connectivity index (θ). First, from the well pressure transient response the spectral dimension was calculated, obtaining the following results (Table 7-4):

Table 7-4: Results from pressure transient response

δ (spectral dimension)	0.54
Case $\delta < 1$:	$d_{mf} < 2$ (flow behavior intermediate between linear and radial).

According to the spectral dimension value, the expected fractal dimension for this case must be less than 2 and the flow regime present in the reservoir is between linear and radial flow. Then according to the methodology proposed in this research, the next step is to apply the rescaled range analysis based on wireline log responses, in order to calculate the fractal dimension, and consequently the connectivity index.

Rescaled range analysis: First, this analysis was based on the sonic well log responses from the upper cretaceous formation, and approximately 1,100 data points were considered. The data was divided in 5 ranges (Table 7-5), where the statistical analysis was

applied (mean and standard deviation) in order to obtain the relationship (R/S); see Chapter 5 for reference.

Table 7-5: Ranges for R/S analysis

R/S	*n* (number of range)
12.8	1
45	2
92.7	3
92.5	4
130.7	5

Second, based on the information showed in Table 7-5, the calculation of the Hurst exponent was based on a log log plot (*R/S vs n*). The slope defined was based on the data related to the reservoir zone in this case upper Cretaceous formation. The slope is called the Hurst exponent, (Figure 7-4).

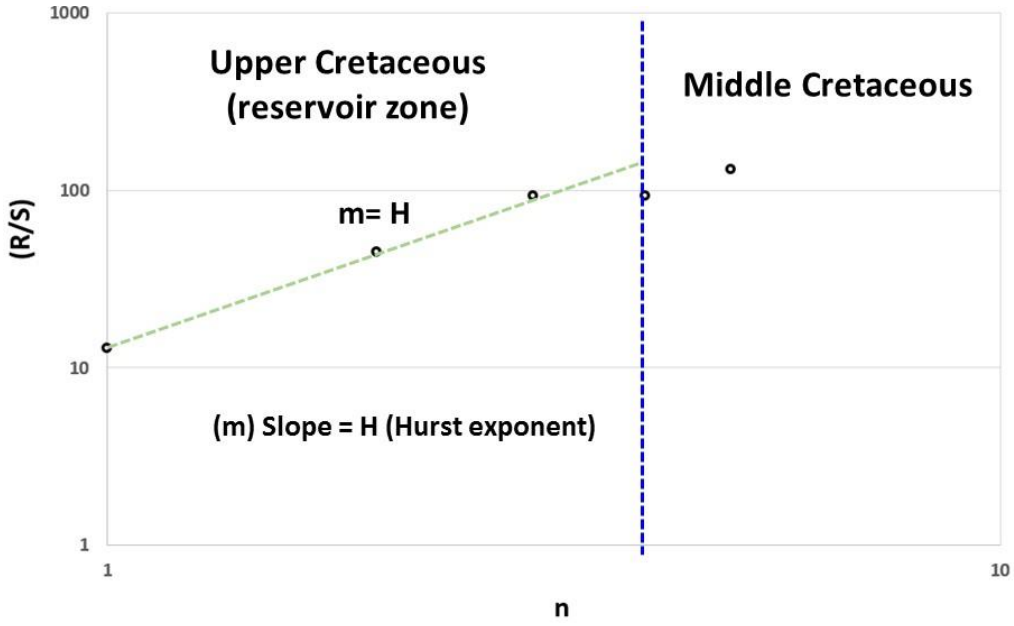

Figure 7-4: Log log plot; R/S versus the number of ranges (Well S-316).

Third, the fractal dimension and connectivity index (θ) were computed based on the methodology proposed; see Table 7-6 for results.

Table 7-6: Fractal parameters

Hurst exponent (H)	0.86
d_{mf}	1.14
θ	0.11

In conclusion, the assumption defined by the calculation of the spectral dimension (δ) from pressure transient response, where d_{mf} is less than 2, was validated. As mentioned before, d_{mf} indicates the fracture density present in the reservoir. To understand the value of d_{mf}=1.14, the fractal network in 2D proposed by Acuna and Yortsos (1995) was used. The

lowest value of d_{mf} was 1.47. Therefore, the fracture density is poor, lower than the worst case presented by Acuna and Yortsos (Figure 4-3). According to the value calculated of d_{mf} for well S-316, the fracture density is really low. Second, the connectivity index is slightly greater than 0 ($\theta=0.11$), which indicates that the fractures are reasonably well connected. Finally, the next step is to evaluate the effect of these parameters on production decline.

Effect of fractal parameters on production decline.

In order to evaluate the effects of fractal parameters on oil rate behavior in well S-316, it was necessary to compare the oil rate from Euclidean geometry wells vs well S-316 with fractal geometry from Campaniano Upper Cretaceous formation, based on a normalized semilog plot ($q/\Delta p$ *(BPD/PSI*) vs *time* (hours), (Figure 7-5).

As expected, the flow rate from the fractal case (well S-316) is smaller than in the Euclidean cases (Wells 334,306,304,314 and 302) in which the diffusion is faster because the fracture density is uniform and all the fractures are connected. On the other hand in the fractal case the oil is produced from finite connected clusters only in a poor fracture density medium.

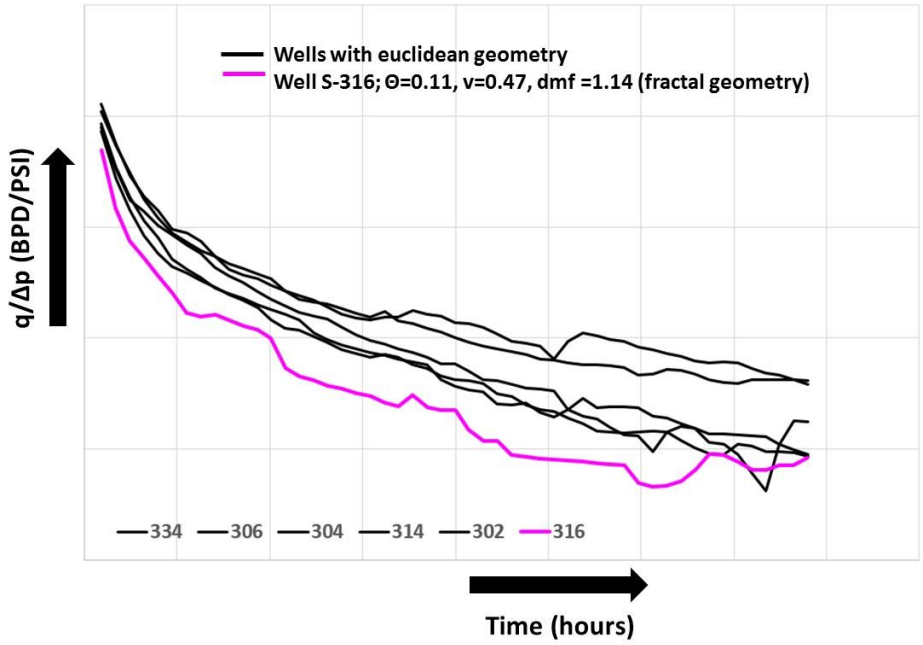

Figure 7-5: Normalized semi log plot (*q/Δp (BPD/PSI*) vs *time* (hours).

7.5 Field case (reservoir AZ)

The field AZ located in the southwest region of Mexico, is a volatile oil reservoir; it includes an average deep of 5,300 meters and is a complex NFR. The formation was deposited during the Upper, Middle and lower Cretaceous. Detailed geological work has identified an average porosity of 9%. Recent well tests and well-logging studies have estimated an average permeability of a value of 8 md. The field only has one well oil producer, which is producing only from the formation Upper Cretaceous (Figure 7-6). The matrix in this field is compact and does not participate in the hydrocarbon production, and therefore, a single porosity analysis was applied.

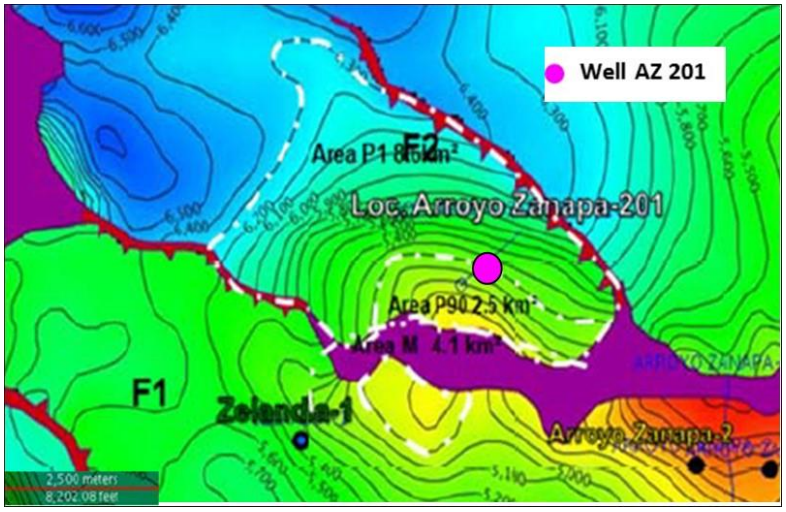

Figure 7-6: Field AZ (Contour map from the formation Upper Cretaceous).

7.5.1 Well AZ-201

Validation of fractal behavior: According to the methodology proposed, the first step was to identify the fractal behavior. Table 7-7 shows the input data for well AZ-201.

Table 7-7: Input data, well AZ-201

Well	**AZ-201**	
h	508.4	ft
Ct	5 exp-5	PSI $^{-1}$
Oil rate	185	stb/d
rw	0.375	ft
API	42	
μ	0.1	cp

Bo	2.8	bbl/stb
Production time before build up test	168	hours

The semi logarithmic derivative technique was applied in order to identify the fractal behavior (Figure 7-7). First, it is important to identify the period of time in the buildup test without production time effects; for this well the production time before the buildup test was 168 hours. It means that only 17 hours from the buildup test is a reliable reservoir response, without production time effects. Second, the validation of the fractal behavior is based on the slopes measured in the log log plot of pressure and pressure derivative versus time. Both of them must be the same and this behavior must remain at last more than ½ cycle in the log log plot. Third, compare the difference between pressure - pressure derivative at a defined time from the log log plot vs the value calculated from the equation: (*1/m*); both of them must be similar (Table 7-8).

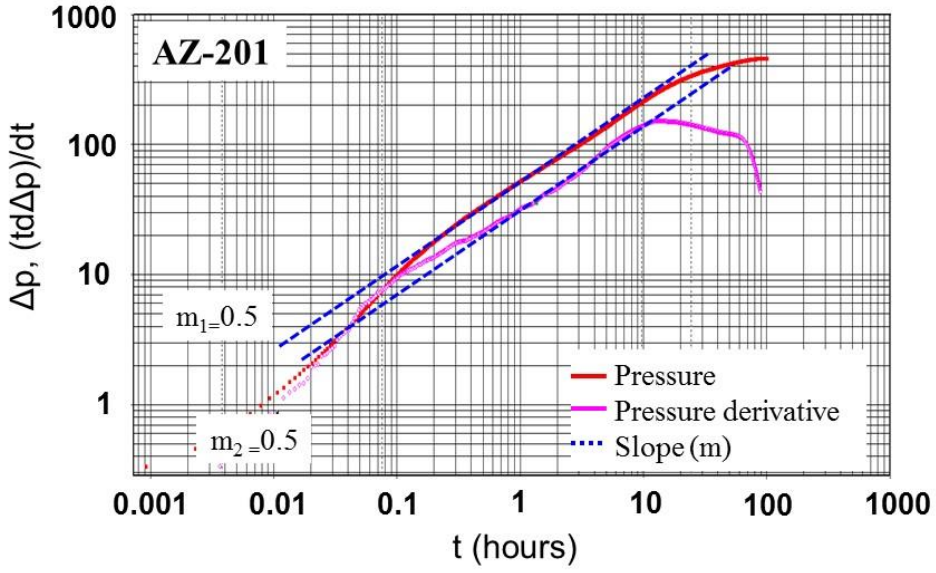

Figure 7-7: Log log plot of pressure and pressure derivative versus time. (Well S-316).

Table 7-8: Results (validation of fractal behavior)

m_1	0.5
m_2	0.5
Log (1/m)	0.30
pressure - pressure derivative @ 1 hour	0.22
Conclusion	**Fractal geometry**

Determination of fractal parameters: Once the fractal behavior was validated, the second step was to calculate the fractal parameters: spectral dimension (δ), fractal

dimension (d_{mf}) and the connectivity index (θ). First, from the well pressure transient response, the spectral dimension was calculated, obtaining the following results (Table 7-9):

Table 7-9: Results from pressure transient response

δ (spectral dimension)	0.50
Case $\delta < 1$:	$d_{mf} < 2$ (flow behavior intermediate between linear and radial).

According to the spectral dimension value, the expected fractal dimension in this case must be less than 2 and the flow regime present in the reservoir is between linear and radial flows. Then according to the methodology proposed in this research; the next step is to apply the rescaled range analysis based on wireline log responses in order to calculate the fractal dimension and consequently the connectivity index.

Rescaled range analysis: First, this analysis was based on the sonic well log responses from the upper Cretaceous formation, and around 2,664 data points were considered. The data was divided in 9 ranges (Table 7-10), where the statistical analysis was applied (mean

and standard deviation) in order to obtain the relationship (R/S); see Chapter 5 for reference.

Table 7-10: Ranges for R/S analysis

R/S	*n* (number of range)
12.8	1
60.1	2
78.7	3
136.2	4
79	5
48	6
46.16	7
27.4	8
28.46	9

Second, based on the information shown, in Table 7-10, the calculation of the Hurst exponent was based on a log log plot (R/S vs n). The slope defined was based on the data related to the reservoir zone, in this case upper Cretaceous formation, the slope is called Hurst exponent see Figure 7-8.

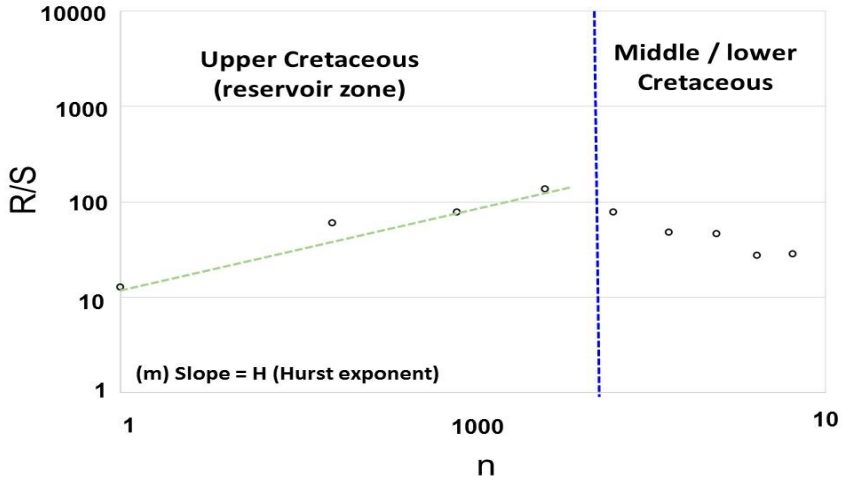

Figure 7-8: Log log plot, R/S versus number of ranges (Well AZ - 201).

Third, the fractal dimension and connectivity index (θ) were computed based on the methodology proposed; see Table 7-11 for results.

Table 7-11: Fractal parameters

Hurst exponent (H)	0.87
d_{mf}	1.12
θ	0.24

As a conclusion, the assumption defined by the calculation of the spectral exponent from pressure transient response, where d_{mf} is less than 2 was validated. As mentioned before, d_{mf} indicates fracture density present in the reservoir, in order to understand the value of d_{mf}=1.12, the fractal network in 2D proposed by Acuna and Yortsos (1995) (Figure 4-3) was used, where the lowest value of d_{mf} was of 1.47. As it can be seen, the fracture density is poor so according to the value calculated of d_{mf} for the well AZ 201 the fracture density

is even poorer than the worst case of Acuna and Yortsos. Second, the connectivity index is greater than 0 ($\theta=0.24$), which means that the fractures are not completely connected between them. Finally, the next step is to know the effect of these parameters on production decline.

Effect of fractal parameters on production decline.

In order to evaluate the effects of fractal parameters on oil rate behavior in well AZ 201, it was necessary to compare the oil rate from an Euclidean geometry well vs AZ 201 with fractal geometry. In this case, there is only one well. For this case the comparison was based on the initial oil rate proposed, based on a Euclidean geometry assumption versus the real oil rate from the fractal geometry reservoir, Figure 7-9.

As expected, the real oil rate is much lower than the expected oil rate calculated based on the Euclidean geometry assumption, in which the diffusion is faster because the fracture density is uniform and all the fractures are connected. On the other hand, in the fractal case, the oil is produced from finite connected clusters only in a poor fracture density medium. This is a very good example where an optimistic forecast was calculated and the fractal parameters were not considered in the decline curve behavior.

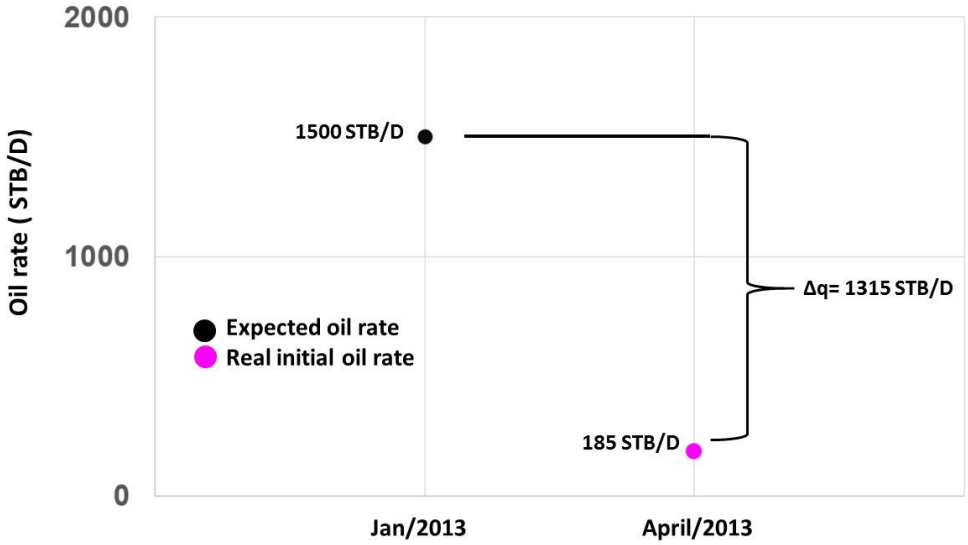

Figure 7-9: Cartesian plot; comparison of expected oil rate and real oil rate (Well AZ-201).

Chapter Eight: **CONCLUSIONS AND RECOMMENDATIONS**

This study contains details of analyzing NFR with fractal geometry and without matrix participation. Two field cases were analyzed with the methodology proposed. The study leads to the following conclusions and recommendations:

- A methodology to identify and analyze NFR with non-Euclidean geometry and no matrix participation is proposed. In this methodology the fractal parameters (d_{mf} and θ) are calculated by the application of a semi logarithmic derivative technique on well pressure transient response, and by the application of the rescaled range analysis based on well logs data. Additionally the permeability and skin factor are computed based on the equations proposed.

- The storage and production time effects must be identified before analyzing any buildup test, in order to validate a reservoir model.

- This study shows that the connectivity between fractures (θ) and fracture density (d_{mf}) play an important role on production performance. The effects of these fractal parameters were validated and analyzed based on dimensionless rate and cumulative production behavior for infinite reservoirs.

- In this study, the methodology proposed was applied to two field cases in order to characterize and understand the production performance.

- If these reservoirs are still treating as reservoirs with Euclidean geometry; a wrong understanding of the fracture density and their connectivity would be obtained, resulting in unproductive wells, very optimistic production forecast and inefficient primary, secondary and enhanced oil recovery methods.

- It is recommended to apply the same methodology in NFR with matrix participation and then evaluate the effects of matrix – fracture coefficients and fractal parameters on the production performance.

- It is also highly recommended to consider the fractal parameters in reservoir simulation models in order to compute realistic production forecasts, and then establish the best strategy to increase the oil and gas recovery factors.

References

1. Acuna J.A., Ershaghi Iraj, SPE, and Yortsos Y.C.: "Practical Application of Fractal Pressure – Transient Analysis in Naturally Fractured Reservoirs." SPE 24705, 1995.
2. Acuna J. A. and Yortsos Y. C.: "Numerical Construction and Flow simulation in Network of fractures using Fractal Geometry." SPE 22703, 1991.
3. Aguilera Roberto: "Integration of geology petrophysics and reservoir engineering for characterization of carbonate reservoirs through Pickett plots, "Servipetrol Ltd, university of Calgary, December 2003.
4. Aguilera Roberto: "Book naturally fractures reservoirs. ", Editorial: PennWell Publishing Company, Tulsa Oklahoma, second edition.1995
5. Aguilera Roberto: "Well Test Analysis of Naturally Fractured Reservoirs, "Servipetrol Ltd, university of Calgary, September 1987.
6. Barenblantt, G.I. and Zheltov, Yu. P. "Fundamentals Equations of Filtration of Homogeneous liquids in Fissure Rocks," Soviet physics, Doklady, 1960.
7. Barton C.C., Scholz C.H., Schutter T.A, Herring P.R., and Thomas W.J., "AAPG Annual Convention," Dallas, Texas, 1991.
8. Beier, R.A.: "Pressure-Transient Model for a Vertically Fractured Well in a Fractal Reservoir," SPE Formation Evaluation, 1994.
9. Camacho-V., R.G., Fuentes-C., G., and Vásquez-C., M.: "Decline Curve Analysis of Fractured Reservoirs with Fractal Geometry," SPE Reservoir Evaluation & Engineering, pp 606-619, June 2008.

10. Camacho-V., R.G., Vásquez-C., M., Castrejón-A., R., and Arana-O., V.: "Pressure-Transient and Decline-Curve Behavior in Naturally Fractured Vuggy Carbonate Reservoirs," SPE Reservoir Evaluation & Engineering, Volume 8, Number 2, April 2005.
11. Capuano, R.M.: "Evidence of Fluid flow in micro fractures in geopressured shale," AAPG Bulletin, 1993.
12. Chang Jincal and Yortsos Yanis C., "Pressure transient Analysis of fractal reservoirs," SPE, U. of Southern California, SPE 18170, 1990.
13. Coalson, E. B., Hartmann, D. J., and Thomas, J. B.: "Productive Characteristics of Common Reservoir Porosity Types," Bulletin of the South Texas Geological Society, v. 15, No. 6, pp. 35-51, February 1985.
14. Coconi-M., E., Ronquillo-J., G., and Campos-E., J.: "Multi-scale analysis of well-logging data in petrophysical and stratigraphic correlation," Geofísica Internacional, 2010, 49 (2), 55-67 (2010), 2009.
15. Crane S.E. and Tubman K.M.: "SPE Paper 20606" SPE Annual Technical Conference, New Orleans, 1990.
16. De Swaan-O.A.: "Analytical Solutions for determining Naturally Fractured Reservoirs Properties by Well Testing," SPE, June 1976.
17. De Swaan-O., A., Camacho-V., R.G., and Vásquez-C., M.: "Interference Tests Analysis in Fractured Formations with a Time-Fractional Equation," SPE 153615, presented at the SPE Latin American and Caribbean Petroleum Engineering Conference, Mexico City, April 2012.

18. Ershaghi Iraj and Rhee Shie-Woo: “Analysis of Pressure Transient Data in Naturally Fractured Reservoirs with Spherical Flow.” SPE 6018, 1976.
19. Feder J.: “Fractals, Plenum Press, New York, 1988.
20. Flamenco-L., F., and Camacho-V., R.G.: “Determination of Fractal Parameters of Fractured Networks Using Pressure-Transient Data,” SPE Reservoir Evaluation & Engineering, Volume 6, Number 1, February, 2003.
21. Friedman, M. and McKiernan, D. E.: “Extrapolation of Fracture Data from Outcrops of The Austin Chalk in Texas to Corresponding Petroleum Reservoirs at Depth,” Journal of Canadian Petroleum Technology, p. 43, October 1995.
22. Hardy H.H, A. Beier Richard “Book Fractals in Reservoir Engineering “World Scientific Publishing Co.Pte.Ltd. 1994.
23. Hewett T.A.: “Fractal Distributions of Reservoirs Heterogeneity and their Influence on fluid Transport,” Chevron Oil field Research Co, SPE 15386, 1986.
24. Hubbert M. King, G. Willis David: “Mechanics of Hydraulic Fracturing,” Washington. D.C. and Atherton, California, 1957.
25. Hurst Harold Edwin, R.P. Black, Y.M. Simaika, Book “Long-term storage: an experimental study,” University of California, 1965.
26. J.L. Mathews, A.S. Emanuel, and K.A Edwards, Petroleum Technology, 1989.
27. Jelmert Aage Tom: “Productivity of Fractal Reservoirs.” SPE 126080, 2009.
28. Kewen Li, Haiyang Zhao: “Fractal Prediction Model of Spontaneous Imbibition Rate, Transport in Porous Media,” Springer Science Business media B.V., 2011.
29. Kuykendall M.D. et al.: “Giant Oil and Gas Fields of the Decade 1990-2000,” Annual Meeting of the AAPG in Denver, Colorado, 1991.

30. Kuykendall, M.D., and Fritz, R.D.: “Misener Sandstone of Oklahoma,” American Association of Petroleum Geologists Search and Discovery Article no. 10018, in Johnson, K.S., ed., Hunton Group, 2001.
31. Lynch M.T. et al.: “Evidence of Paleokarstification and Burial Diagenesis in the Arbuckle Group of Oklahoma,” Oklahoma State University, 1990.
32. Mandelbrot Benoit: “Book The Fractal Geometry of Nature. “International Business Machines Thomas j. Watson research center, Editorial: W.H. Freeman and company, New York, 1977, 1982 and 1983.
33. Mandelbrot Benoit & Wallis James R.: “Computer experiments with fractional Gaussian noises,” Water Resources Research: 5, 1969.
34. Martin, A. J. et al.: “Characterization of Petrophysical Flow Units in Carbonate Reservoirs,” AAPG Bulletin, v. 83, no. 7, p. 734-759, May 1997.
35. McNaughton, D.A.: “Dilatancy in Migration and Accumulation of Oil in Metamorphic Rocks,” American Association of Petroleum Geology Bulletin, 1953.
36. McNaughton, D. A. and Garb, F. A.: “Finding and Evaluating Petroleum Accumulations in Fractured Reservoir Rock,” Exploration and Economics of the Petroleum Industry, v.13, Matthew Bender & Company Inc., 1975.
37. Mead, W.J.: “The Geologic Role of Dilatancy,” Journal of Geology, 1925.
38. Najurieta, H.L.: “A theory for Pressure Transient Analysis in Naturally Fractured Reservoirs,” JPT, July 1980.
39. Nelson, R.A.: “Fracture Permeability in Porous reservoirs, an Experimental and Field Approach,” Ph.D. Dissertation, Texas A&M University, 1975.

40. Nelson, R.A.: “Geologic Analysis of Naturally Fractured reservoirs,” Gulf Publishing, Houston, Texas, 1985.
41. Nelson, R.A.: “Geologic Analysis of Naturally Fractured Reservoirs, Contributions in Petroleum geology and engineering,” Vol. 1, Gulf Publishing Co., Houston, Texas, 1985.
42. Olarewaju, J.S.: “Modeling Fractured Reservoirs with Stochastic Fractals,” SPE 36207 International Petroleum Exhibition and Conference, Abu Dhabi, 1996.
43. Pang J. and North C.P.: “Fractals and their Applicability in Geological Wireline Log Analysis, “Journal of petroleum Geology, Vol 19(3), pages 339-350, July 1996.
44. Pingping Shen, Mingxin Liu and Fenshu Jia.: “Application of Fractal Techniques in Reservoir Development.” SPE 50878.1998.
45. Poon D.: “Transient Pressure Analysis of Fractal Reservoirs., “The petroleum Society of CIM, paper 96-35, 1995.
46. Raghavan, R.: “A note on the drawdown, diffusive behavior of fractured rocks, Water Resources Research, V. 45, 2. 2009.
47. Restrepo Dora Patricia: “Analisis de Registros Verticales de Porosidad y su Aplicacion al Modelamiento fractal de un yacimiento, “Posgrado de Recursos Hidraulicos de la Universidad Nacional de Colombia, Chapters 5 and 6, August 2000.
48. Sahimi Muhammad and Yortsos Yanis C.: “Applications of Fractal Geometry to Porous Media: A Review.” University of Southern California, SPE 20476, 1990.

49. Serra, K.V., Reynolds, A.C., and Raghavan, R.:"New Pressure Transient Analysis Methods for Naturally Fractured Reservoirs," JPT, October 1983.
50. Stearns, D. W.: "AAPG Fractured Reservoirs School Notes," Great Falls, Montana, 1982-1994.
51. Stearns, D.W., and M. Friedman.: "Reservoirs in Fractured Rock," American Association of Petroleum Geology", Memoir 16, 1972.
52. Warren, J, E. and Root, P.J. "The behavior of Naturally Fractured reservoirs," SPE, September 1963.
53. Xiang Kong, Daolun Li and Detang Lu: "Transient pressure analysis in porous and fractured fractal reservoirs," Department of Mechanics & Mechanical Engineering, University of Science and Technology of China, 2009.